Spatial Scaling of Land Use/Land Cover And Ecosystem Services Across Urban Hierarchical Levels: Patterns And Relationships

Xiao Sun
Chinese Academy of Agricultural Sciences
Qun Ma (maqun0127@shnu.edu.cn)
Shanghai Normal University

Research Article

Keywords: Ecosystem services, Land use/land cover, Scaling relations, Urban agglomeration, 44 Urban hierarchical levels

Posted Date: May 6th, 2021

DOI: https://doi.org/10.21203/rs.3.rs-425853/v1

Version of Record: A version of this preprint was published at Landscape Ecology on January 31st, 2022.
See the published version at https://doi.org/10.1007/s10980-021-01387-4.

Spatial scaling of land use/land cover and ecosystem services across urban hierarchical levels: Patterns and relationships

Xiao Sun, Qun Ma*

Xiao Sun
Key Laboratory of Agricultural Remote Sensing (AGRIRS), Ministry of Agriculture and Rural Affairs/Institute of Agricultural Resources and Regional Planning, Chinese Academy of Agricultural Sciences, Beijing 100081, China
Email: sunxiao@caas.cn

Xiao Sun
State Key Laboratory of Urban and Regional Ecology, Research Center for Eco-Environmental Sciences, Chinese Academy of Sciences, Beijing 100085, China

Qun Ma*
School of Environmental and Geographical Sciences, Shanghai Normal University, Shanghai 200234, China
Email: maqun0127@shnu.edu.cn

Abstract

Context Land use/land cover (LULC) patterns seriously affect the ecosystem services (ESs), especially in highly developed urban agglomerations. Exploring how LULC and ESs change spatially across urban hierarchical levels and understanding the possible mechanisms can promote the sustainable planning of urban landscapes.

Objectives By mapping the spatial patterns of LULC and ESs in three largest urban agglomerations of China, this study aimed to (1) identify the scaling relations of LULC and ESs across different urban hierarchical levels, (2) explore the possible mechanisms of these two types of spatial scaling, and (3) explore how the scaling relations of ESs response to LULC and its policy implications.

Methods Based on LULC, we used the Integrated Valuation of Ecosystem Services and Tradeoffs (InVEST) model and other biophysical models to quantify ES indicators. Then, scalograms were used to quantify the scaling relations of LULC and ESs with respect to changing spatial extent.

Results Developed land and cropland exhibited the most predictable responses with changing spatial extent. Compared to other ESs, provisioning services were the most predictable. The predictable scaling relations of ESs at different urban hierarchical levels fell into two general types: power laws at the city proper level and exponential relationships at the metropolitan region and urban agglomeration levels.

Conclusions The scaling relations of both LULC and ESs varied across urban hierarchical levels. The spatial scaling of ESs was closely related to LULC patterns. Integrating the scaling relations of ESs into land use planning can help decision-makers formulate multi-scale landscape conservation strategies.

Keywords Ecosystem services · Land use/land cover · Scaling relations · Urban agglomeration · Urban hierarchical levels

Introduction

For the past few decades, many parts of the world have been undergoing dramatic and rapid urbanization (Stokes and Seto, 2019). As the world's most populous country, China has also experienced dramatic urban expansion and socioeconomic development since the national reform and opening up policies of 1978 (Chen et al. 2020; Liu et al. 2020). Various studies have used population density (Normile 2016; Poku-Boansi 2021) or built-up land area (Seto et al. 2012; Xu et al. 2018) to represent or measure urbanization. The urbanization population rate in China increased from 17.9% in 1978 to 59.6% in 2018 (Wu et al. 2020), and the urban land area expanded from 21,770 km^2 to 74,827 km^2 in the same period (Kuang 2020a). This rapid urbanization has caused dramatic changes in land use/land cover (LULC) compositions and structures with high spatial heterogeneity (Hasan et al. 2020; Lawler et al. 2014). As the basis of assessing ESs, LULC changes have resulted in myriad impacts on natural resources and further threatening ESs from a local to global scale, such as with water scarcity (Li et al. 2020), climate change (Patra et al. 2018), soil erosion (Hu et al. 2019), and habitat loss (Swenson and Franklin 2000). Studying how LULC and ESs change spatially in rapidly urbanizing regions is important for better understanding and predicting the patterns and processes of urbanization across multiple scales, and the findings may further benefit urban sustainable planning and ecological protection (Batty 2008; Wu et al. 2011; Zhao et al. 2018b).

Previous studies have explored the spatial characteristics of LULC patterns and ESs (Hasan et al. 2020; Viglizzo et al. 2012). However, we still lack further information about the spatial scale effects of LULC and ESs, and their underlying mechanisms. The hierarchical scaling strategy provides an effective method of investigating spatial heterogeneity of complex urban systems over a range of scales (O'Neill et al. 1986; Wu 1999; Wu and David 2002). First, urban systems exhibit a hierarchically structured system wherein large urban regions consist of individual cities, which in turn consist of a smaller city proper (Ma et al. 2019). Thus, the hierarchical perspective can systematically characterize the impacts of landscape patterns on ecological processes in urban regions (Bian et al. 2020; Ma et al. 2016b; Zhang et al. 2020b). Second, the scaling approach is a powerful tool that can quantify multiscale characteristics explicitly and describe how various urban attributes scale with city size (Bettencourt 2013; Lobo et al. 2020).

Until now, the scaling approach has predominantly been used to focused on two themes: The first theme is how urban metrics (e.g., physical, demographic, economic, or environmental attributes) change within city sizes (usually represented by the population size or urban area) (Brock 1999; Fuller and Gaston 2009; Zhao et al. 2018a). Previous studies illustrated that most urban attributes follow approximate power law scaling, with different scaling exponents (e.g., >1 for certain quantities reflecting wealth creation and innovation and <1 for certain material infrastructural quantities) (Bettencourt et al. 2007; Bettencourt et al. 2010; Ribeiro et al. 2020). The second theme is how landscape patterns (e.g., landscape shape) or ecological processes (e.g.,

the relations between impervious surface area and land surface temperature) change with spatial scale (e.g., grain size or extent). For example, Wu (2004) systematically investigated the responses of landscape metrics to changing scale and classified the responses into two categories: simple scaling functions and unpredictable behavior. In general, most of the existing studies have focused on landscape patterns (Kedron et al. 2018; Wu et al. 2004; Zhang et al. 2009) but neglected to explore the scaling relations of ecological process and ES indicators. In the studies on landscape patterns, researchers rarely investigate the specific scaling relations for different LULC types. Especially, it is still unclear how the scaling relations of different LULC types and multiple ESs change in rapidly urbanized regions with a hierarchical structure.

Urban agglomeration is a highly developed spatial form of integrated cities and exhibits a hierarchically structured system (Ma et al. 2019; Wang et al. 2019b). As urban complex systems, urban agglomerations are suffering the most serious changes in terms of LULC and ESs (Shen et al. 2020; Yu et al. 2019; Zhou et al. 2018). Thus, we selected the top three urban agglomerations in China, the Beijing-Tianjin-Hebei (BTH), the Yangtze River Delta (YRD), and the Pearl River Delta (PRD) areas (Du et al. 2018), to explore the spatial features of LULC and ESs. The scaling evolutions of various LULC types and ESs can help to predict or speculate the indicator values, from one scale to another unknown scale (Xu et al. 2020). In addition, understanding the possible processes and mechanisms behind the scaling functions of urban metrics is helpful for guiding land use management and sustainable policy practice at different urban hierarchical levels globally.

This study used the hierarchical scaling strategy to investigate how different LULC types and ESs change within the spatial extent of the three largest urban agglomerations in China. We aimed to achieve the following research objectives: (1) analyze the scaling relations of LULC and ESs across different urban hierarchical levels; (2) understand the underlying mechanisms behind the scaling relations of LULC and ESs; and (3) explore how the scaling relations of ESs respond to LULC and its policy implications.

Methods

Study area

The top three urban agglomerations, BTH, YRD, and PRD (Fig. 1), cover only 5% of Chinese territory (DUSNB, 2019) but generate 40% of the total national urban impervious surface (Ma et al. 2019). They are the primary carriers of China’s socioeconomic development and new urbanization processes (Fang and Yu 2017). In 2018, BTH, YRD, and PRD accounted for 8.1%, 11.0%, and 5.1% of the total national urban population and 9.5%, 16.7%, and 9.2% of the total gross domestic product (GDP), respectively (DUSNB 2019). In addition to their importance to China's economic and social development, these three urban agglomerations constitute the typical and core regions of prominent environmental issues in China (Zhang et al. 2017; Gao et al. 2019).

Administrative urban hierarchy is the most common and actual ecosystem management

boundary for regional planning and policy implementation (Forgione et al. 2016; Nikodinoska et al. 2018; Xing et al. 2021). BTH, YRD, and PRD consist of mature and complete nested urban hierarchical levels that extend from the city proper, metropolitan region to the broader urban agglomeration (Ma et al. 2019). The lowest city proper level (the city proper of Beijing, Shanghai, or Guangzhou) belongs to a metropolitan region (Beijing, Shanghai, or Guangzhou metropolitan region), and is also embedded in the highest urban agglomeration level (BTH, YRD, or PRD urban agglomeration) (Fig. 1).

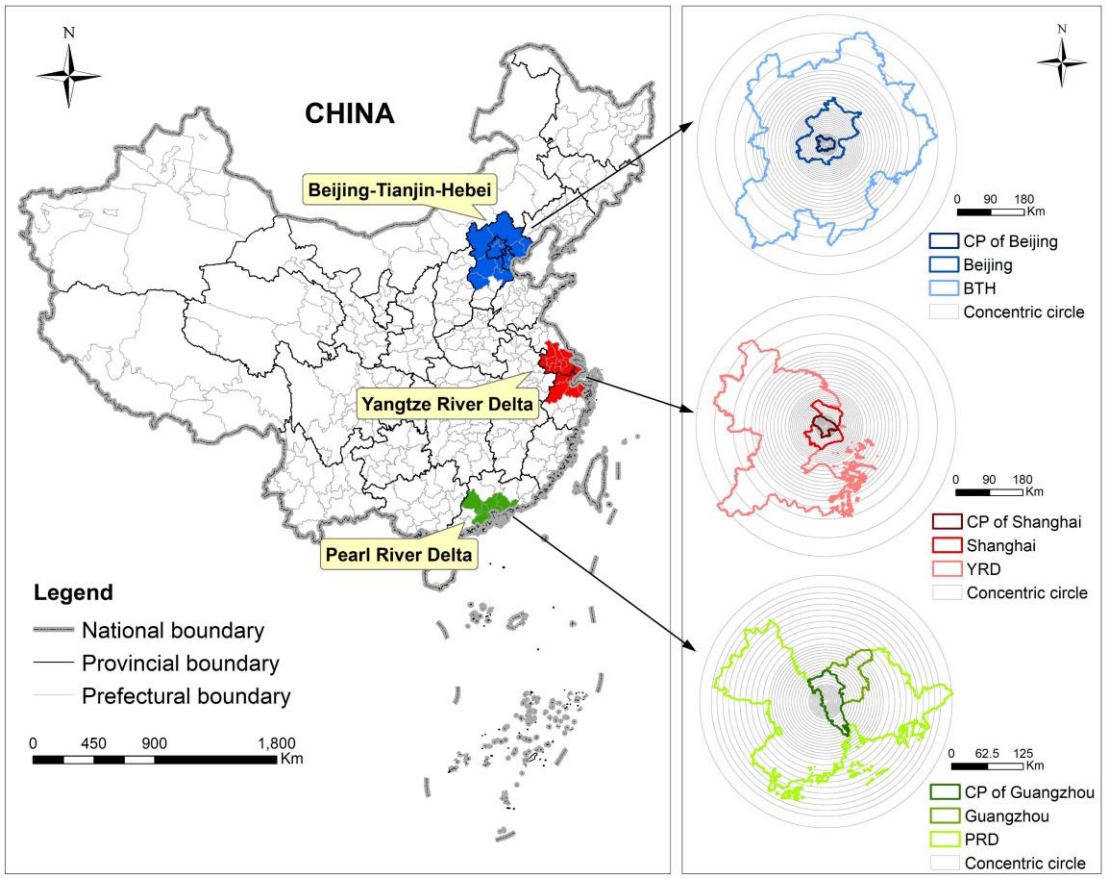

Fig. 1 Location and administrative hierarchy of study areas. The concentric circle illustrations on the right represent the spatial extension of three urban agglomerations at the administrative hierarchy levels. The CP of Beijing/Shanghai/Guangzhou refer to the city proper of Beijing/Shanghai/Guangzhou; Beijing/Shanghai/Guangzhou refer to the Beijing/Shanghai/Guangzhou metropolitan region; BTH/YRD/PRD refer to the Beijing-Tianjin-Hebei/Yangtze River Delta/Pearl River Delta urban agglomeration.

Data acquisition

For the three urban agglomerations, LULC data with a spatial resolution of 30 × 30 m in 2018 were downloaded from the Resource and Environment Science and Data Center (http://www.resdc.cn/). Digital elevation model data with a spatial resolution of 30 × 30 m were derived from the Geospatial Data Cloud (http://www.gscloud.cn/). Climate data, including the

annual average precipitation and temperature in all meteorological stations, were collected from the China Meteorological Data Service Center (http://data.cma.cn/). Potential evapotranspiration data were collected from the Global Aridity and PET Database (https://cgiarcsi.community/data/global-aridity-and-pet-database/). Soil properties data, including bulk density, soil organic carbon, clay content, sand content, silt content, and soil depth, were obtained from the World Soil Information database (https://soilgrids.org/).

LULC maps in urban agglomerations

LULC maps in 2018 for the BTH, YRD, and the PRD urban agglomerations were generated by researchers at the Institute of Geographic Sciences and Natural Resources Research, Chinese Academy of Sciences, through manual visual interpretation. The original data were Landsat 8 OLI_TIRS remote-sensing images that were downloaded from the United States Geological Survey (https://www.usgs.gov/). The raster data comprised six LULC types: (1) cropland, including irrigated cropland, dry cropland, and orchards; (2) forests, including natural forests, artificial forests, coppice, shrub forests, and sparse forests; (3) grassland, including all types of grasslands with coverage of more than 5%, pastures, and hay; (4) water bodies, including rivers, lakes, reservoirs, ponds, swamps, tidal lands, and wetlands; (5) developed land, including urban construction land, rural residential land, industrial land, traffic road, airport, and mining area; and (6) barren land, including sandy land, desert, saline land, swampland, bare land, bare rock, and other unutilized lands.

Quantifying multiple ES indicators in urban agglomerations

This study selected eight ES indicators: carbon storage, food production, water yield, air pollution removal, nitrogen retention, soil retention, habitat quality, and recreational opportunity. The selection was based on three criteria: (1) the indicators belong to the basic provisioning, regulating, and cultural services (Millennium Ecosystem Assessment 2005); (2) they have great significance to the sustainable development of three urban agglomerations (Liu et al. 2018; Luo et al. 2020; Sun et al. 2018; Zhang et al. 2017); and (3) they can comprehensively reflect the characteristics of complex urban ecosystems and represent the information of water resources, food, climate, soil, habitat, and culture in urban agglomerations.

We used the Integrated Valuation of Ecosystem Services and Tradeoffs (InVEST) model to quantify the carbon storage, water yield, nitrogen retention, soil retention, and habitat quality for the three urban agglomerations. Food production was estimated by using the Global Agro-Ecological Zones (GAEZ) model. The removal of $PM_{2.5}$ (atmospheric aerosol particles with a diameter of less than 2.5 μm) was estimated on the basis of the adsorption capacity of vegetation to $PM_{2.5}$ pollutants. Recreational opportunity was quantified by the Recreation opportunity Spectrum (ROS) model. Table 1 listed the ES indicators and assessment descriptions. In addition, the calculation process and detailed parameters were shown in Supplementary Information (SI).

178 **Table 1**

179 Descriptions of ecosystem service (ES) indicators and the assessment methods

ES types	Principles and descriptions of ES assessment models
Carbon storage	The InVEST Carbon Storage and Sequestration model maps the carbon densities of different land use/land cover (LULC) types and summarizes the results into aggregate storage values (Goldstein et al. 2012).
Food production	The food production potential was calculated by considering the limiting factors, such as water resource, soil properties, topographic conditions, cultivated land distribution, and management measures (Liu et al. 2015).
Water yield	The InVEST Water Yield model estimates the water of different landscape areas. It is based on the principle of water balance on a grid map (Sharp et al. 2020).
$PM_{2.5}$ removal	The $PM_{2.5}$ removal was calculated on the basis of the adsorption of $PM_{2.5}$ per unit area for different LULC types.
Nitrogen retention	The InVEST Nutrient Delivery Ratio model assesses nitrogen retention according to the nutrient pollutants removed by vegetation and soil in surface runoff (Sharp et al. 2020).
Soil retention	The InVEST Sediment Delivery model computes sediment retention based on the amount of soil loss and its delivery ratio (Hamel et al. 2015).
Habitat quality	The InVEST Habitat Quality model combines the information of LULC types and threats to biodiversity to produce habitat quality maps (Sharp et al. 2020).
Recreational opportunity	The ROS model was associated with the recreational index and accessibility index for reaching the recreational locations (Lavorel et al. 2020).

180

181 *Quantifying the scaling relations of LULC and ESs with respect to spatial extent*

182 ES supply depends on ecosystem structures and processes. Thus, LULC change has become a
183 major driving force that impacts regional ecosystem change (Hasan et al. 2020). Both LULC
184 compositions and configuration are expected to significantly impact ESs (Lei et al. 2021).
185 Therefore, exploring how LULC change responds to increased spatial extent is an important basis
186 for understanding and explaining the spatial scaling effect of ESs. The form of scalograms (Frazier
187 2016; Ma et al. 2019; Wu 2004) was adopted in this study to reflect how different LULC types
188 and ESs respond to changing spatial extents in three urban agglomerations. A series of concentric
189 circles with gradually expanding radii were used to represent the expansion of spatial extent across
190 urban hierarchical levels (Fig. 1, Table 2). The spatial extent was expressed as the radius of a
191 concentric circle. Thus, scalograms were constructed by plotting the changes of LULC and ESs
192 with respect to increasing spatial extents (Wu 2004).

193

Table 2

The radii list of concentric circles at different administrative hierarchical levels for BTH, YRD, and PRD urban agglomerations (Unit: km).

BTH urban agglomeration			**YRD urban agglomeration**			**PRD urban agglomeration**		
CP of Beijing	Beijing	BTH	CP of Shanghai	Shanghai	YRD	CP of Guangzhou	Guangzhou	PRD
4	4	4	4	4	4	4	4	4
6	6	6	6	6	6	6	6	6
8	8	8	8	8	8	8	8	8
10	10	10	10	10	10	10	10	10
12	12	12	12	12	12	12	12	12
14	14	14	14	14	14	14	14	14
16	16	16	16	16	16	16	16	16
18	18	18	18	18	18	18	18	18
20	20	20	20	20	20	20	20	20
22	22	22	22	22	22	22	22	22
24	24	24	24	24	24	24	24	24
26	26	26	26	26	26	26	26	26
28	28	28	28	28	28	28	28	28
30	30	30	30	30	30	30	30	30
	35	35	35	35	35	35	35	35
	40	40	40	40	40	40	40	40
	45	45		45	45	45	45	45
	50	50		50	50	50	50	50
	55	55		55	55	55	55	55
	60	60		60	60	60	60	60
	65	65		65	65	65	65	65
	70	70		70	70	70	70	70
	75	75			75		75	75
	80	80			80		80	80
	85	85			85		85	85
	90	90			90		90	90
	95	95			95		95	95
	100	100			100		100	100
	110	110			110		110	110
	120	120			120		120	120
	130	130			130			130
		140			140			140
		150			150			150
		160			160			160
		170			170			170
		180			180			180
		190			190			190
		200			200			200
		220			220			220
		250			250			
		300			300			
		350			350			

Note: The center of concentric circles is the administrative center of a city proper. For each urban hierarchical level, the concentric circle with the maximum radius can cover the boundary of the corresponding level. BTH/YRD/PRD represents the Beijing-Tianjin-Hebei/Yangtze River Delta/Pearl River Delta urban agglomeration, CP of Beijing/Shanghai/Guangzhou refers to the city proper of Beijing/Shanghai/Guangzhou.

Using SPSS 25.0, we adopted the curve estimation regression models (Jomnonkwao et al. 2020) to investigate the scaling relations. The coefficient of determination (R^2) was used to indicate the goodness of fit of the curve (Massada and Radeloff 2010). The independent variable (X) was the radius of the concentric circle (spatial extent). The dependent variable (Y) was the proportion of LULC or the average ES value within the corresponding concentric circle area.

Results

Scaling relations of LULC for three urban agglomerations

For the three urban agglomerations, proportions of developed land decreased as the spatial extent increased. In contrast, the proportions of forests and cropland increased with the expansion of the spatial scale. The proportion of water bodies showed irregular fluctuations with the expansion of scale. In addition, the proportion of grassland in BTH increased when the spatial scale expanded. Further, the proportions of grassland and barren land were exceedingly small in YRD and PRD (Fig. 2, Fig. 3).

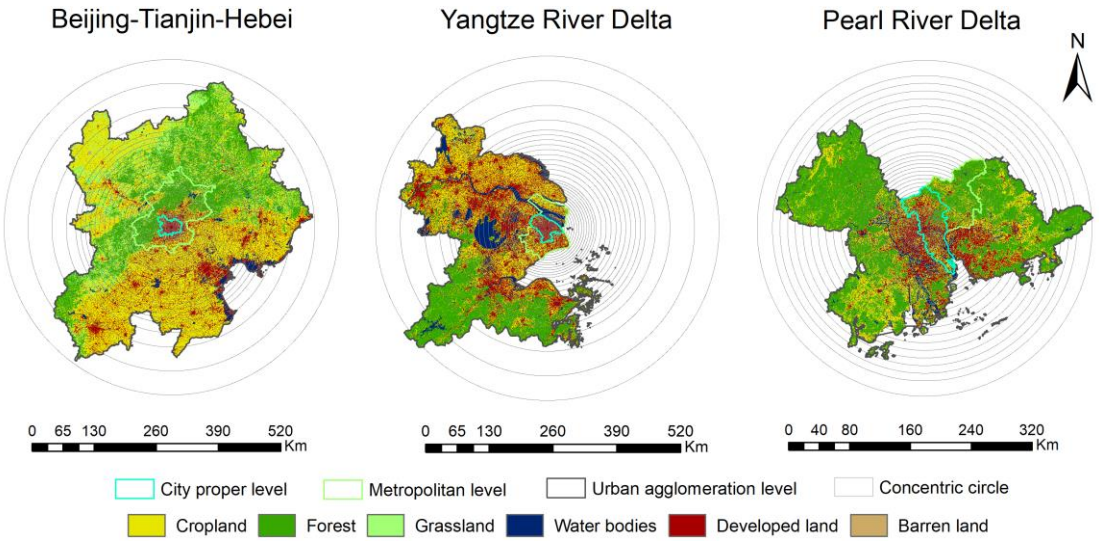

Fig. 2 Spatial distributions of land use/land cover in 2018 for three urban agglomerations. The radii list of concentric circles is shown in Table 2.

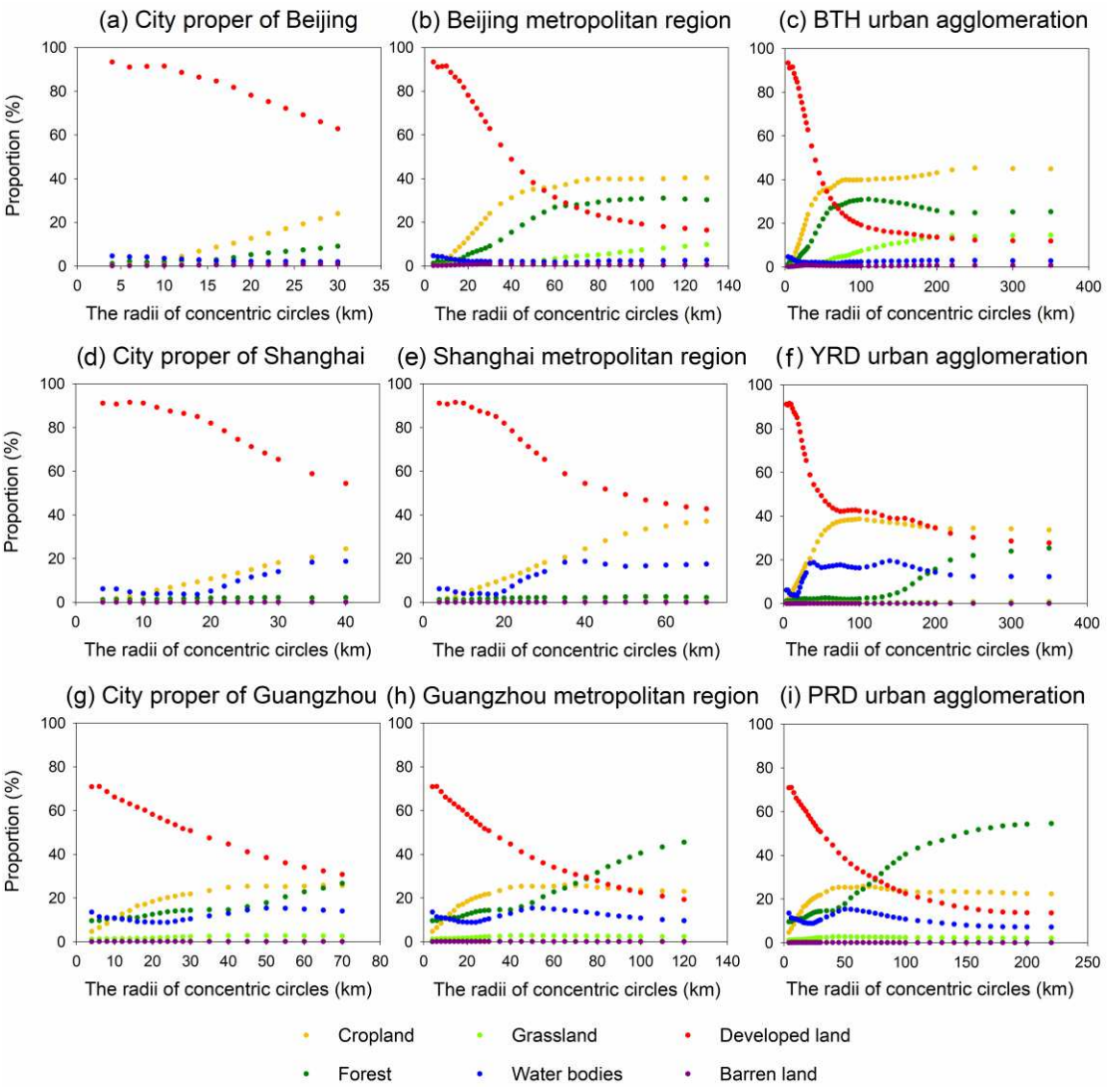

Fig. 3 Scalograms of the proportion of different land use/land cover types with respect to increasing concentric circle radii in the three largest urban agglomerations of China (Beijing-Tianjin-Hebei (BTH), Yangtze River Delta (YRD), and Pearl River Delta (PRD)).

Overall, the proportions of cropland, forest, and developed land exhibited appropriate and predictable scaling laws at certain levels of urban hierarchy. The typical scaling curves for different urban hierarchical levels were classified into three rules: linear, sigmoidal, and exponential relationships. Among them, the exponential relationships were divided into exponential growth and exponential decay (Fig. A1). However, the scaling relations of water bodies and barren land were unpredictable at nearly all three urban hierarchical levels. The proportion of grassland showed scaling laws in BTH, but this was unpredictable in YRD and PRD (Table 3).

For the BTH area, the linear scaling relations were found at the city proper level for most of the land use types. Next, the general relationships were converted into exponential and sigmoidal functions at the broader metropolitan and urban agglomeration levels. For YRD, most of the

LULC types did not reveal the scaling relations and functions except for cropland and developed land. Both showed linear relationships at the city proper level and sigmoidal and exponential growth or exponential decay at higher urban hierarchical levels, respectively. For PRD, the cropland, forest, and developed land scaled in a predictable way. The proportions of cropland increased with exponential curves, while forest increased with sigmoidal curves. The proportions of developed land decreased in a linear relationship at the city proper level, while it converted to exponential decay at the higher levels (Table 3).

Table 3

Type of scaling relations for proportions of different land use/land cover with respect to increasing radii of concentric circles within the three largest urban agglomerations

Urban agglomeration	Land use/land cover types	Urban hierarchical levels		
		City proper	Metropolitan region	Urban agglomeration
Beijing-Tianjin-Hebei	Cropland	Linear	Sigmoidal	Exponential growth
	Forest	Linear	Exponential growth	–
	Grassland	Linear	Exponential growth	Sigmoidal
	Water bodies	Exponential decay	–	–
	Developed land	Linear	Exponential decay	Exponential decay
	Barren land	Linear	–	–
Yangtze River Delta	Cropland	Linear	Sigmoidal	Exponential growth
	Forest	–	–	Sigmoidal
	Grassland	–	–	–
	Water bodies	–	–	–
	Developed land	Linear	Exponential decay	Exponential decay
	Barren land	–	–	–
Pearl River Delta	Cropland	Exponential growth	Exponential growth	Exponential growth
	Forest	Sigmoidal	Sigmoidal	Sigmoidal
	Grassland	Sigmoidal	–	–
	Water bodies	–	–	–
	Developed land	Linear	Exponential decay	Exponential decay
	Barren land	–	–	–

Note: The archetypes of scaling relations were shown in Fig. A1. For all scaling relation equations in Table 3, the relationships between the proportions of land use/land cover types and the increasing spatial extents were significant (**$P<0.001$, $R^2>0.990$).

Scaling relations of multiple ESs in BTH

For the spatial patterns of multiple ESs in BTH, the values for most of ESs become higher with increasing spatial extent, except for water yield and soil retention (Fig. 4). According to the scalograms of multiple ESs, with respect to increasing spatial extent in BTH, the carbon storage, food production, water yield, $PM_{2.5}$ removal, nitrogen retention, and the habitat quality revealed significant and predictable scaling relations at different urban hierarchical levels. However, the soil retention did not show any scaling relations. In general, the two form functions, which were power law and exponential functions, can fit the scaling relations of ESs better in the BTH

agglomeration. The ESs showed pervasive power law scaling relations at the city proper level while exhibiting exponential scaling relations at the higher metropolitan and urban agglomeration levels (Fig. 5).

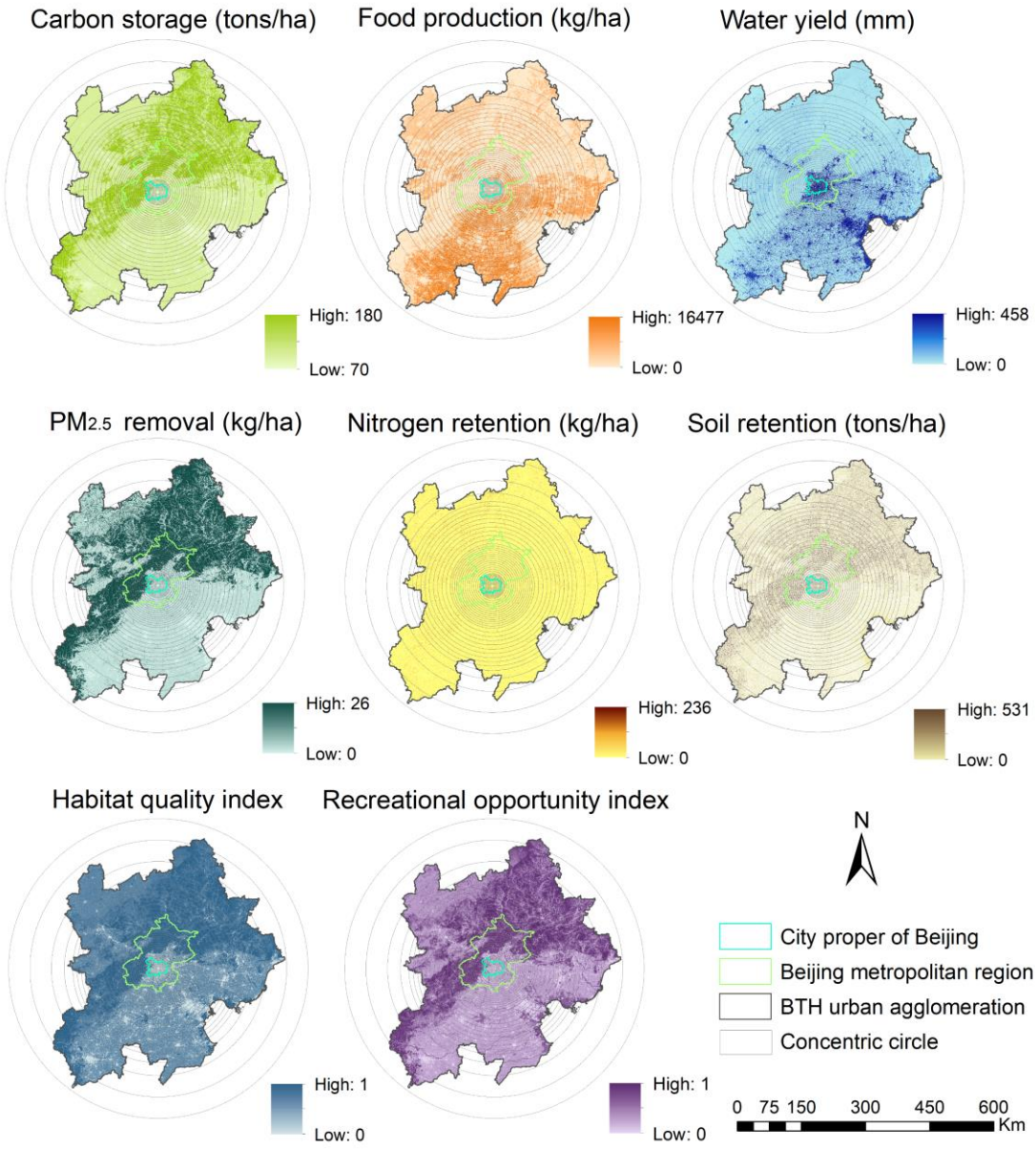

Fig. 4 Spatial distributions of multiple ecosystem services in 2018 for Beijing-Tianjin-Hebei (BTH) urban agglomeration. The radii list of concentric circles was shown in Table 2.

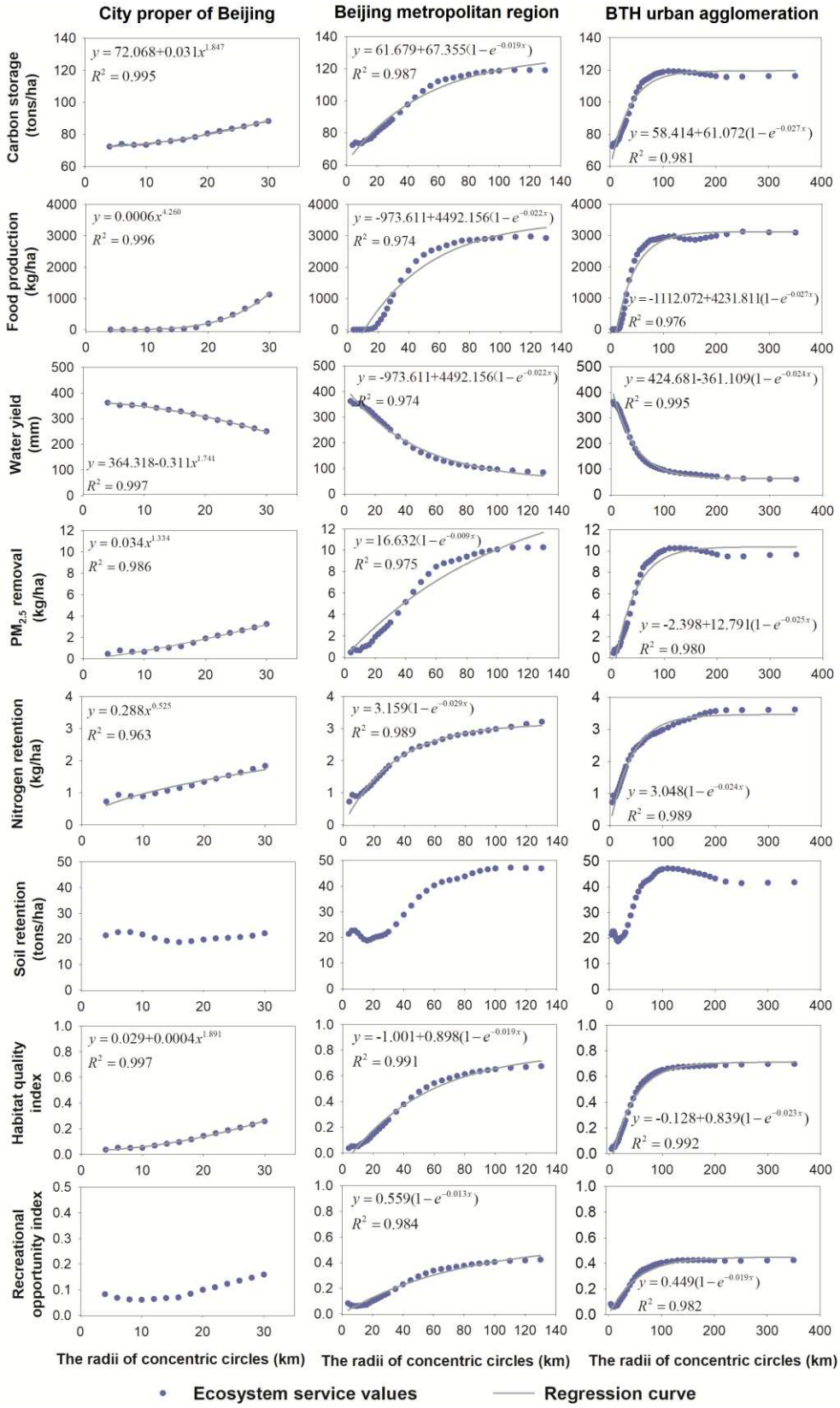

Fig. 5 Scalograms of multiple ecosystem service indicators with respect to increasing concentric circle radii at various urban hierarchical levels: the city proper of Beijing, Beijing metropolitan region, and the Beijing-Tianjin-Hebei (BTH). For all regression curves and equations, the significance level P-values < 0.001.

Specifically, the values of carbon storage, food production, $PM_{2.5}$ removal, and habitat quality increased consistently and followed a power law function with a scaling exponent of greater than 1 within the city proper of Beijing. As the spatial extent increased in the metropolitan region and urban agglomeration, the indicator values showed exponential functions with negative exponents. For nitrogen retention, the scaling exponent was smaller than 1 in the power law function within the city proper of Beijing. As the spatial extent increased beyond the city proper, the nitrogen retention values also showed an exponential function with a negative exponent and continued to increase until it eventually remained stable. In addition to these increasing indicators, the water yield showed a decreasing trend with the expansion of spatial extent. The index values followed a power law decline within the city proper of Beijing. They continued to decrease with exponential scaling relations at higher urban hierarchical levels. For recreational opportunities, the index values first decreased and then increased with the increasing spatial extent within the city proper. As the spatial extent increased, the index values followed exponential functions and continued to grow until it stabilized (Fig. 5).

Scaling relations of multiple ESs in YRD

For the spatial patterns of multiple ESs in YRD, the values for most of ESs become higher with increasing spatial extent, except for water yield, nitrogen retention, and soil retention (Fig. 6). According to the scalograms of multiple ESs of the increasing spatial extent in YRD, only food production and water yield displayed universal and predictable scaling relations at different urban hierarchical levels. For carbon storage, $PM_{2.5}$ removal, and habitat quality, the index values followed predictable scaling relations within the Shanghai metropolitan region. As the spatial extent further increased beyond the metropolitan region, the scaling relations became unpredictable. In addition, for nitrogen retention, soil retention, and recreational opportunities, there were no predictable scaling relations that could fit the curves (Fig. 7).

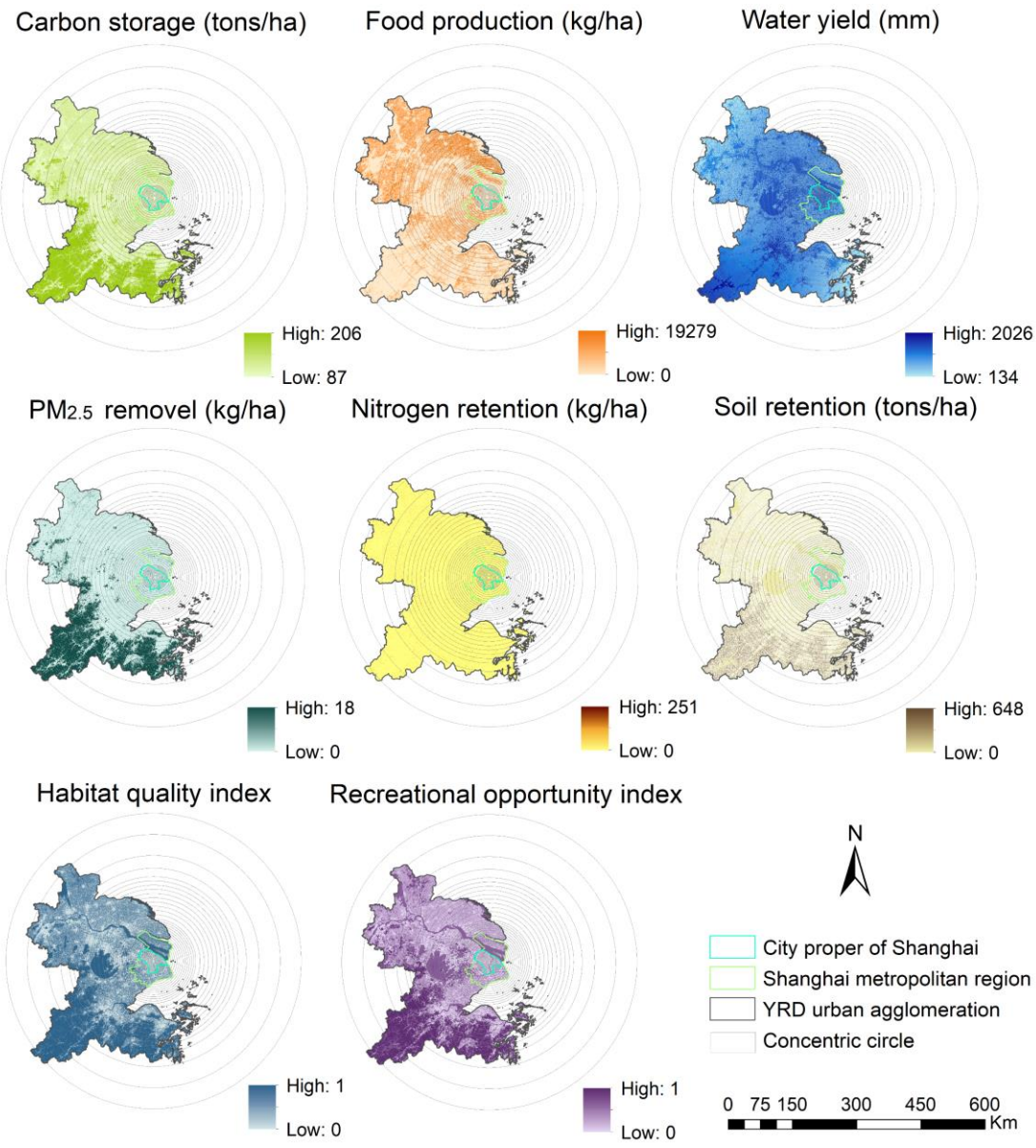

297

298 **Fig. 6** Spatial distributions of multiple ecosystem services in 2018 for Yangtze River Delta (YRD)

299 urban agglomeration. The radii list of concentric circles was shown in Table 2.

300

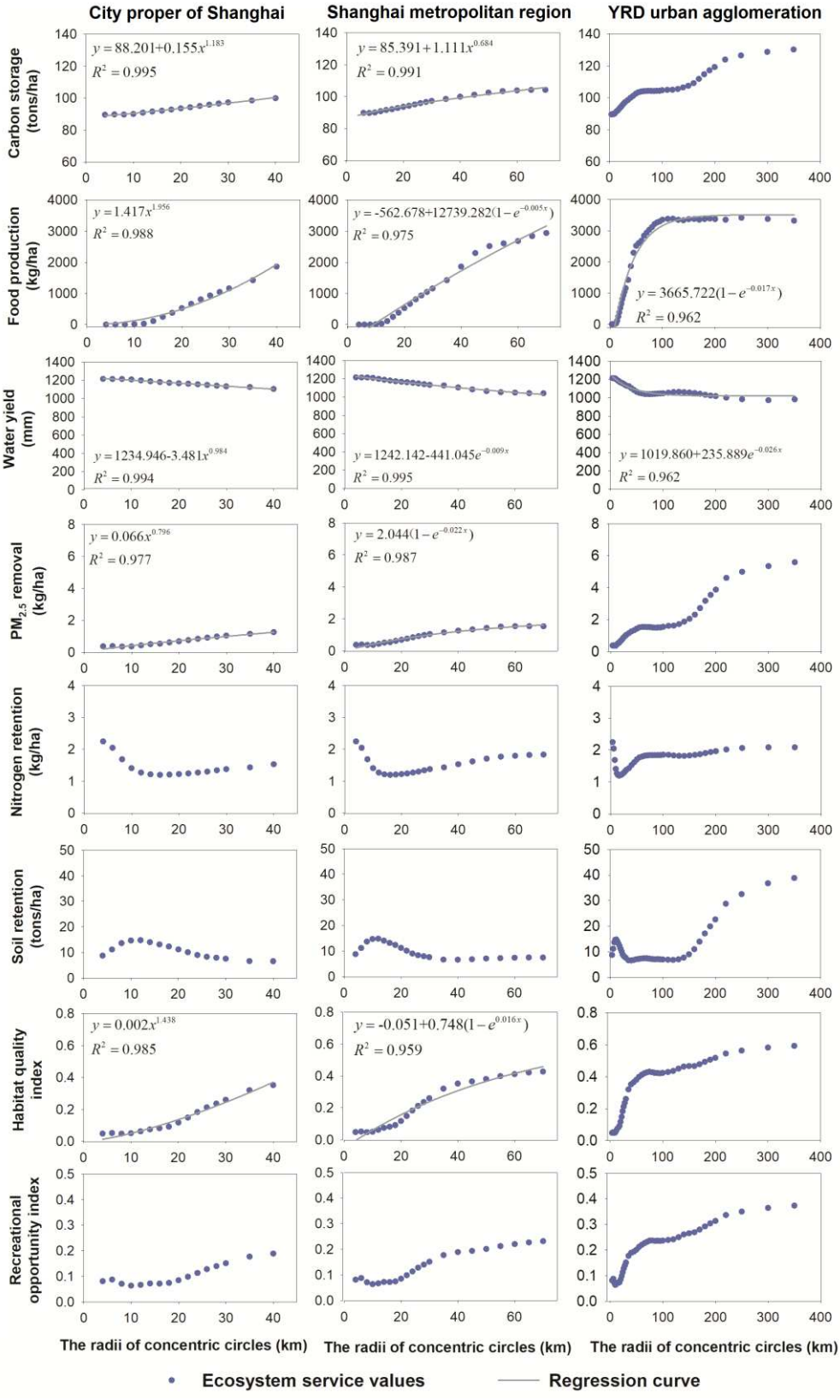

Fig. 7 Scalograms of multiple ecosystem service indicators with respect to increasing concentric circle radii at various urban hierarchical levels: the city proper of Shanghai, Shanghai metropolitan region, and the Yangtze River Delta (YRD). For all regression curves and equations, the significance level P-values < 0.001.

Specifically, food production values increased with a power law scaling relationship at the city proper level, while it showed exponential growth scaling relationships at higher urban hierarchical levels. Water yield values decreased with a power law scaling relation at the city proper level, followed by exponential decay scaling as the spatial extent covered the metropolitan region and urban agglomeration. For carbon storage, $PM_{2.5}$ removal, and habitat quality, the index values exhibited power law scaling relations within the city proper of Shanghai. As the spatial extent further increased to the Shanghai metropolitan region, carbon storage still followed a power law function, while $PM_{2.5}$ removal and habitat quality followed an exponential growth relationship. The values of these three ESs showed upward staircase-like curves when the spatial extent increased to urban agglomeration. In addition, the values of nitrogen retention did not change significantly at various urban hierarchical levels. The soil retention values performed best when spatial extent increased beyond the metropolitan region. The recreational opportunity index values showed an upward staircase-like curve with increasing spatial extent (Fig. 7).

Scaling relations of multiple ESs in PRD

For the spatial patterns of multiple ESs in PRD, the values for most of ESs become higher with increasing spatial extent, except for water yield and soil retention (Fig. 8). According to the scalograms of multiple ESs, with respect to increasing spatial extent in PRD, the carbon storage, food production, water yield, $PM_{2.5}$ removal, nitrogen retention, and habitat quality all exhibited predictable scaling relationships at different urban hierarchical levels. As with the BTH agglomeration, the scaling relationships of soil retention in PRD were unpredictable. The recreational opportunity showed a predictable scaling relation only at the urban agglomeration level. In general, the scaling relationship also presented two types of functions, which were power law and exponential relationships. Moreover, exponential relationships predominantly existed at higher urban hierarchical levels (Fig. 9).

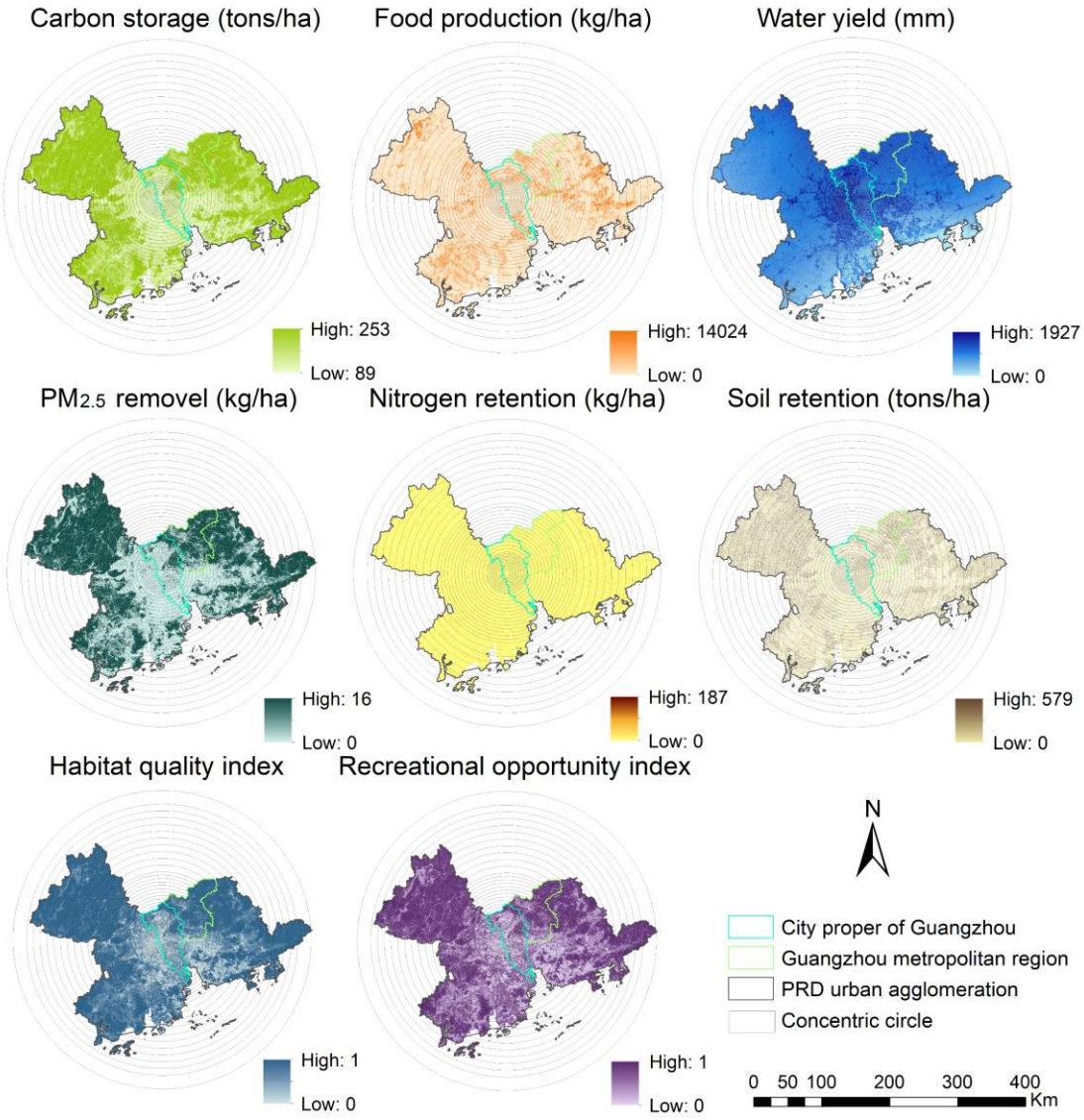

331

332 **Fig. 8** Spatial distributions of multiple ecosystem services in 2018 for Pearl River Delta (PRD)
333 urban agglomeration. The radii list of concentric circles was shown in Table 2.

334

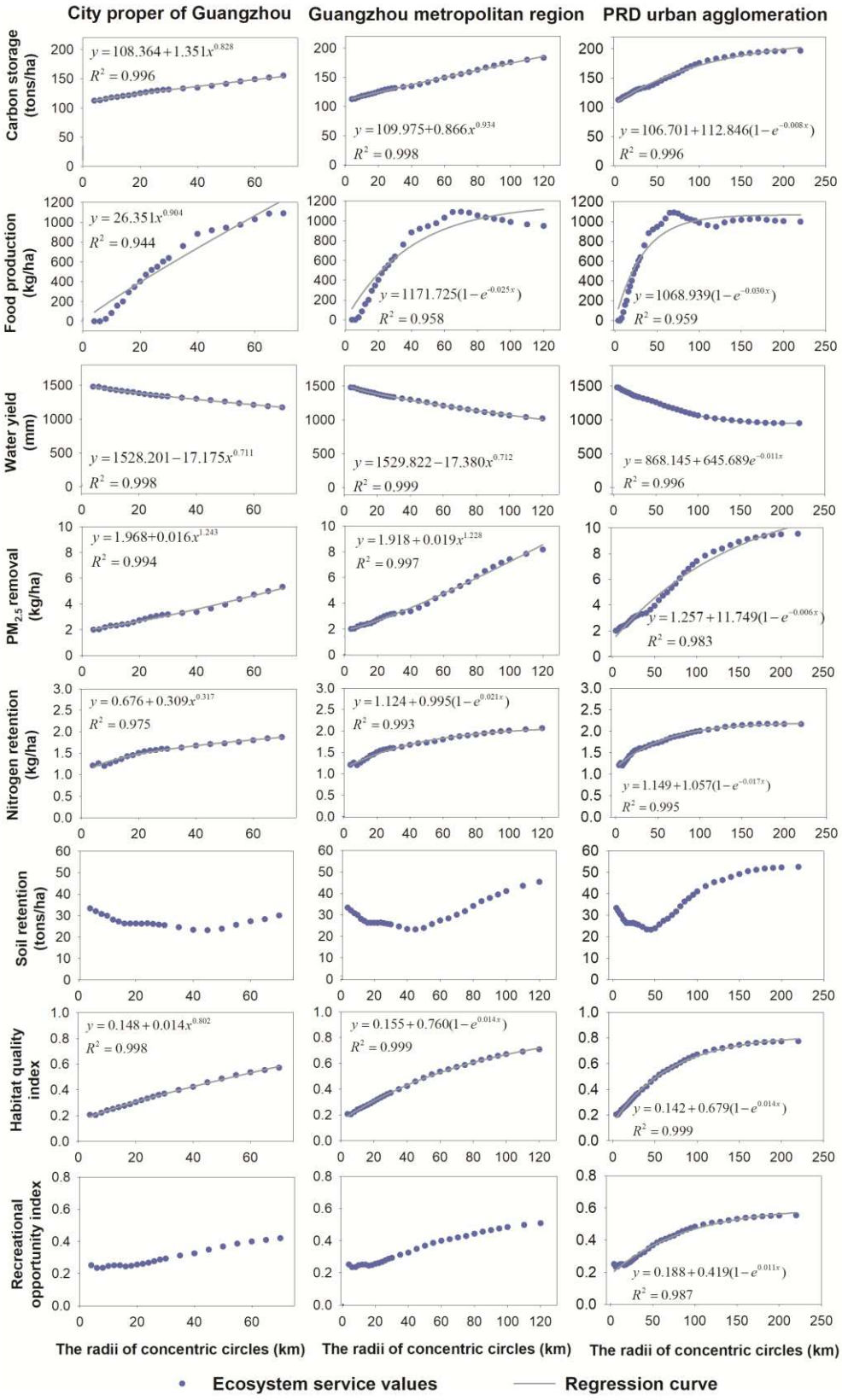

Fig. 9 Scalograms of multiple ecosystem service indicators with respect to increasing concentric circle radii at various urban hierarchical levels: the city proper of Guangzhou, Guangzhou metropolitan region, and the Pearl River Delta (PRD). For all regression curves and equations, the significance level P-values < 0.001.

Carbon storage and $PM_{2.5}$ removal values followed power law functions within the Guangzhou metropolitan region. Thereafter, they showed exponential functions as the spatial extent further increased to the urban agglomeration. The values of food production, nitrogen retention, and habitat quality followed power law functions within the city proper and then increased exponentially as the spatial extent increased beyond the city proper. For water yield, the index values showed a monotonously decreasing trend as the spatial extent increased. The index values followed the power law functions within the Guangzhou metropolitan region and then showed the exponential function as the spatial extent increased. For recreational opportunity, the index values began to follow an exponential function only when the spatial extent increased to the urban agglomeration level (Fig. 9).

Discussion

How did the scaling relations of LULC change across different urban hierarchical levels and agglomerations?

Different LULC types showed diversified distribution trends when the spatial extent increased. The developed lands exhibited decreasing trends from city proper outwards when croplands and forests showed an increasing trend. This was mainly because croplands and forests were substantially occupied by developed land during the rapid process of urbanization in China, especially for large urban agglomerations (Zhou et al. 2021; Kuang et al. 2020b). In contrast, water bodies and grasslands showed irregular and random characteristics with the increase of spatial extent. This phenomenon was predominantly related to natural geographical conditions (e.g., topography, climate, etc.), regional planning (e.g., park layouts, the demarcation of nature reserves), and other socioeconomic factors (Luo et al. 2020; Sun et al. 2020; Yang et al. 2019). In addition, barren lands had no obvious scaling relations, as its area within the three highly urbanized agglomerations was exceedingly small.

Among all LULC types, developed land and cropland were the most predictable at three urban hierarchical levels (Table 3). Developed land and cropland were most severely affected by human activities, especially in urban centers (d'Amour et al. 2016). Socioeconomic factors such as population agglomeration and gross domestic product growth predominantly affect the spatial pattern of developed land and cropland (Arcaute et al. 2015; Gu 2019; Li et al. 2017). The scaling relations of socioeconomic factors can be well approximated by common laws. For example, since the population density and the Gross Domestic Product followed predictable functions in the three urban agglomerations (Fig. A2), the two LULC types were also spatially predictable. The predictable scaling relationships of this study can provide information for the extrapolation of developed lands and croplands at different spatial amplitudes and urban hierarchical levels.

Different urban hierarchical levels presented various scaling relationships for LULC, of which the city proper level was the most predictable. For example, water bodies and barren land showed predictable scaling functions at the city proper level but were unpredictable at the broader

metropolitan and urban agglomeration levels (Table 3). This was predominantly because the influencing factors of LULC distributions became more diverse with the gradual expansion of spatial amplitude (i.e., the addition of more natural, geological, and policy factors, such as topography, climate, and regional planning) (Du et al. 2014; Verburg et al. 2003). This made the scaling relationships more complex and increased unpredictability. At the city proper level, linear relationships (i.e., power law with scaling exponent = 1) existed for most of the LULC types. The results were relatively consistent with those of previous studies, showing that developed lands followed power law scaling relationships with increasing extent in highly urbanized areas (Ma et al. 2019). In urban centers, human production and living activities severely disturbed the land spatial composition. Previous studies have proved that high population densities mainly influenced the spatial patterns of urban developed lands within the city proper (Ma et al. 2016a; Ma et al. 2019). As the spatial extent increased to broader metropolitan and urban hierarchical levels, population densities became smaller and more stable and showed exponential decay functions at the urban agglomeration level (Fig. A2). Thus, human disturbances gradually weakened outside the suburbs (Lan et al. 2021; Liu et al. 2018). This led to the change rates of developed land and cropland slow down and the corresponding regression curves became exponential rules at the broader scales (Fig. 3; Table 3).

Different urban agglomerations also presented various scaling relationships for LULC, among which the relations in BTH were the most predictable and those in YRD were the weakest. This was related to the development modes of urbanization in the agglomerations. BTH was a simple combined urban agglomeration, with Beijing as the core metropolitan area and Tianjin as the sub-core city. PRD contains core cities concentrated in the central region while YRD was a more complex urban agglomeration with several dispersed core cities (Fig. 2) (Fang and Yu 2017). Especially for YRD, the spatial patterns of different LULC presented complex and unpredictable scaling relations. The main reasons were as follows: (1) the city proper of Shanghai can only expand westward due to topography conditional constraints (Fig. 1) and (2) YRD is a spatial polycentric mega-city region (Chen et al. 2019), which led to the fragmentation of forest, croplands, and other landscape patches (Lu et al. 2018). This kind of polycentric pattern was induced by a series of regional integration development measures. For example, the General Office of the State Council, PRC, proposed the “Regional Plan for Yangtze River Delta Region” in 2010 (www.gov.cn/) and implemented equal infrastructure construction, industrial planning, and public service popularization in each core city, which aggravated polycentric development.

How did the scaling relations of multiple ESs change and response to LULC across different urban hierarchical levels and agglomerations?

Most ES values increased with the increasing spatial extent, except for water yield, nitrogen retention, and soil retention in three urban agglomerations. The average values of carbon storage, $PM_{2.5}$ removal, habitat quality, and recreational opportunity were lower in urban centers and

414 became higher in broader metropolitan and urban agglomeration regions, due to the increase of
415 ecological lands, such as forests, wetlands, and grasslands (Fig. 2). Previous studies have shown
416 that ecological land per unit can provide more similar regulation and cultural services, compared
417 to artificial land (Baumeister et al. 2020; Luo et al. 2018). In contrast, the values of water yield
418 were highest in urban centers. This was mainly because the reference evapotranspiration in urban
419 areas was less than in suburban vegetated areas (Benra et al. 2021; Yang et al. 2019). It is worth
420 noting that soil retention changed irregularly with increase in spatial extent. The phenomenon was
421 largely determined by comprehensive factors, such as topography (Sun et al. 2014), rainfall
422 intensity (Rodríguez-Caballero et al. 2013), and vegetation distribution (Korkanç and Dorum
423 2019).
424 For different types of ESs, provisioning services were most predictable. The food production
425 and water yield showed predictable scaling relations at all hierarchical levels and urban
426 agglomerations. For example, food production revealed power law and exponential growth
427 relationships at all three urban agglomerations. Landscape structure (e.g., composition and
428 configuration) was often considered linked to ecological processes and ESs (Botequillha Leitao
429 and Ahern 2002). To be specific, the scaling relations of food production in this study might be
430 associated with the predictable distribution of croplands. Both food production and croplands
431 increased rapidly on smaller scales (power law functions) and became stable at larger urban
432 agglomeration scales (exponential functions). In addition, some types of regulating ESs only
433 exhibited predictable functions at certain urban levels, such as for carbon storage and $PM_{2.5}$
434 removal within YRD (Fig. 7). When the spatial scale extended to the broader urban hierarchical
435 levels, the scaling relationships of these two indicators transformed into complex staircase-like
436 patterns. A previous study has shown that the scalograms of urban impervious surfaces exhibited
437 scale breaks (change points) that corresponded roughly to the urban administrative levels (Wu and
438 Li 2006). Similar to urban impervious surfaces, the breakpoint changes also existed in croplands,
439 forests, and developed lands (Fig. 3f), which might cause the staircase-like patterns of carbon
440 storage and $PM_{2.5}$ removal within YRD.
441 Different urban hierarchical levels presented two types of scaling functions for ESs, among
442 which the power laws predominantly expressed ES patterns at smaller levels while exponential
443 relationships were more suitable for larger levels. Although the power law function was found to
444 be ubiquitous when representing the scaling relationship between ecological attributes and
445 measurable scales (Fisher et al. 2008; Newman 2005; Spence 2004), it cannot fully express the
446 scaling results of LULC and ESs for various types and urban hierarchical levels. Zhao and Liu
447 (2014) found that a similar power law relationship existed in the critical scale resolution of the
448 carbon cycle with spatial extent. They proposed that future studies should further investigate the
449 compatibility of power law with the scaling relations of ecological indicators. This study fills the
450 research gap in the scaling of ESs and demonstrates that power law scaling can be fitted well only
451 at certain ranges or urban hierarchical levels. At the city proper level, landscape structures were

often shaped by anthropogenic factors that were related to developed lands, such as demographic, economic, and traffic (Li et al. 2013; Ma et al. 2019; Xie et al. 2017). Consequently, the ESs revealed similar predictable power law functions that were consistent with developed lands. As the spatial extent increased to broader metropolitan or urban agglomeration regions, cropland, forest, and other ecological lands were incorporated into dominant LULC types (Fig. 3). Natural factors, such as topography and climate conditions, which are macroscopic and stable, became the main driving forces in shaping landscape patterns and processes (Peng et al. 2017; Smith et al. 2019). Thus, the ES patterns became stable and exhibited significant exponential relationships on a broader scale.

Different urban agglomerations also presented various scaling relationships for ESs, among which the BTH was the most quantitatively predictable while the YRD was unpredictable. The study showed that the more complicated the distribution of LULC, the greater the variability of ES patterns (Yee et al. 2021) and the poorer the predictability of scaling relations. Therefore, the predictability of spatial scaling of ESs may be closely related to the complexity of LULC patterns. Compared with YRD and PRD, the distribution shape of BTH was more regular and the LULC area was spread evenly in all directions of concentric circles (Fig. 1). The urbanization of BTH was dominated by the "urban edge-expansion mode (the newly developed patches expanded from the fringes of existing urban centers)" (Jia et al. 2020), which made ESs more scale-predictable. However, the scaling relations of ESs in YRD were difficult to predict for the following two key reasons: (1) the topographical constraints and polycentric urban development had complicated the urban shape and increased landscape fragmentation (Li and Zhou 2019; Tao et al. 2020), and thus intensified the spatial heterogeneity of ESs. (2) Large proportions of ESs were provided by forest and water bodies in YRD; however, these two LULC types were unpredictable (Table 3), which also affected the predictability of spatial scaling of ESs.

How to integrate the scaling relations of ESs into land use planning and policy practice?

The results of this study confirmed that the scaling of ESs were closely related to the land use patterns in urban agglomerations. Thus, the supply of multiple ESs can be effectively improved by managing the spatial patterns of LULC (Mitchell et al. 2015). The most vulnerable and the worst performing area for multiple ESs was the city proper, the key human dominated region (Robinson et al. 2009). It thus required land use optimization. At the city proper level, LULC patterns were more predictable, and thus, the planning can promote ESs more predictably. However, urbanization expansion and LULC spatial patterns emerged from a myriad of policy decisions and planning processes (Batty 2008). To conserve ESs, diversified land management measures should be implemented to avoid disorderly or leapfrog urban expansion. First, more compact urban expansion forms should be encouraged, such as improving land use efficiency to maintain rational densification (Shoemaker et al. 2019; Wang et al. 2019a). Second, conserving the natural land cover, such as by setting the "ecological red line" to protect green and blue spaces in urban areas

(Lin and Li 2019), can effectively improve regulating and cultural services. Specifically, the priorities are to reconcile the conflict between developed land and cropland in the city proper of Beijing while protecting those ecological lands that are affected by urbanization most seriously, such as water bodies in the city proper of Shanghai and forests in the city proper of Guangzhou (Fig. 3) (Wang et al. 2020; Zhang et al. 2020a). Third, decision-makers can adjust landscape structures by optimizing landscape configuration (Rieb and Bennett 2020), promoting landscape connectivity, and using other measures to support the landscape multifunctionality (Bolliger et al. 2011) and increase the supply of ESs per unit area.

The scaling relations of ESs could reflect the actual spatial characteristics of the ecological environment at each urban hierarchical level of the urban agglomerations. We used piecewise function to simulate the scaling curve of ESs, which can reflect the critical thresholds (change points) of various ES indicators (Momblanch et al. 2016) that were the turning points of the change rates of scaling relations for ESs (Fig. 10a). The range of change point represents the actual geographical boundary of the ES scaling changes, which was not consistent with the urban administrative boundary. Fig. 10b and Fig. 10c illustrate the distance (variance) between the change point of ES scaling relations and the administrative boundary for multiple ESs in the three urban agglomerations. In the city proper, the change point values for most of the ESs were larger than the boundary value of the city proper of Beijing, while the change point values for all ESs were less than the boundary value of the city proper of Guangzhou. This reflected that the eco-environmental effects of urbanization of Beijing city proper had gone beyond the scale of administrative planning, and hence, the actual management extent of ESs should be broader than the administrative boundary. In contrast, the eco-environmental effects of urbanization for Guangzhou city proper had not extended to the administrative boundary, and the actual impact extent of ESs were smaller than the administrative boundary. At the metropolitan level, the actual impact extent of most of the ESs was broader than the administrative boundary in the Shanghai metropolitan region, while the actual ES boundaries were smaller in the Beijing and Guangzhou metropolitan regions. The urban sprawl and polycentric development in the Shanghai metropolitan region (Tao et al. 2020) had exceeded the administrative boundary. Therefore, the Shanghai metropolitan region should pay more attention to the impacts of urbanization on ESs. To effectively protect the ecological environment and natural resources, policy makers should incorporate the actual extent of ES management into sustainable land use planning, rather than merely relying on administrative boundaries (Brunet et al. 2018; Hein et al. 2006). This means that the proposed ES boundary changes can provide a theoretical basis for the boundary determination of the actual natural resource management and landscape planning in urban agglomerations.

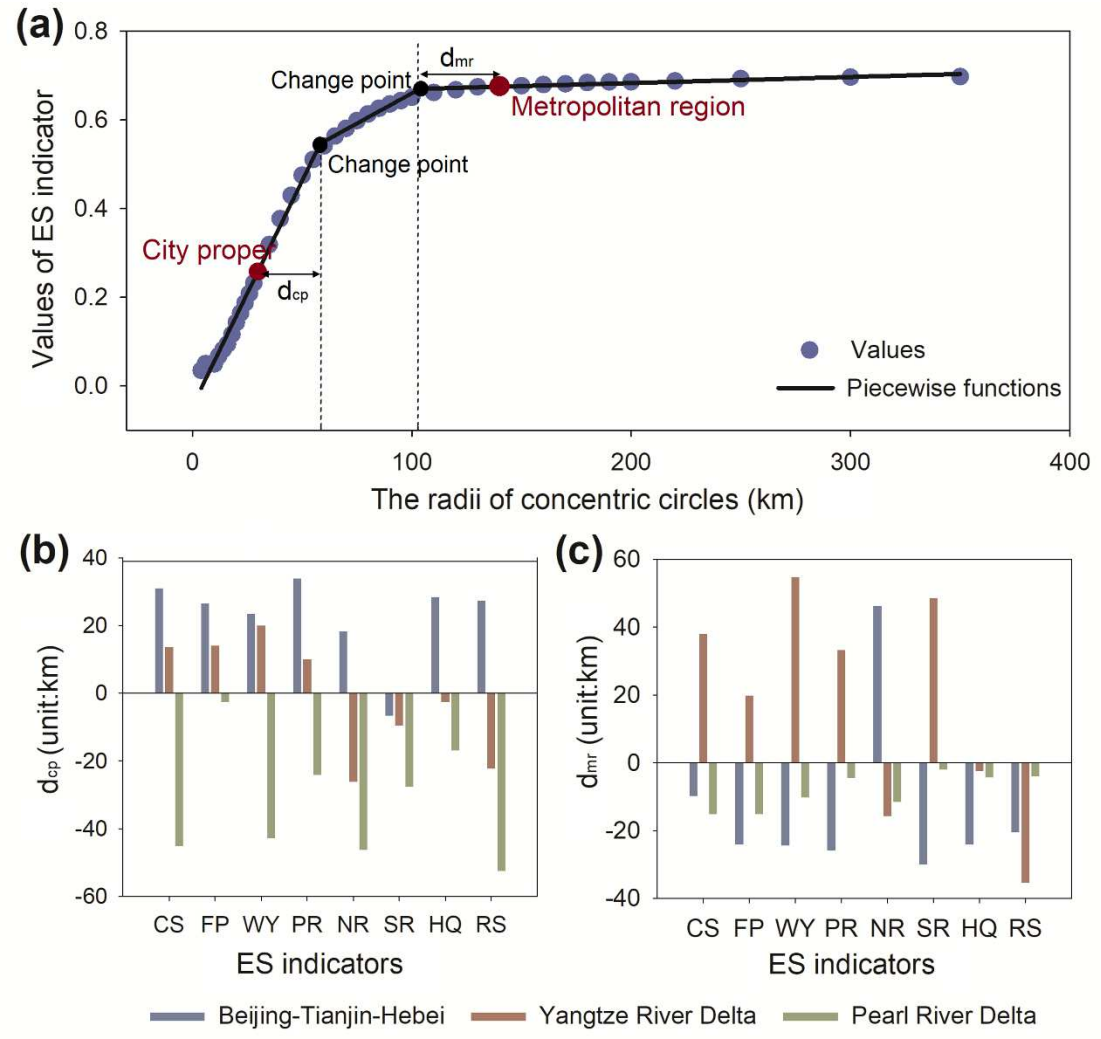

Fig. 10 (a) Example of a scalogram for ecosystem service (ES) change points versus the administrative boundary points. The solid black dots represent the turning points for the ES change rates; the solid red dots represent the administrative boundary points. The "d_{cp}" represents the distance between the first change point of ES scaling relations and the administrative boundary of the city proper; the "d_{mr}" represents the distance between the second change point of ES scaling relations and the administrative boundary of the metropolitan region. Distance was calculated by the change point value minus the administrative boundary value. **(b)** The "d_{cp}" for multiple ESs in Beijing-Tianjin-Hebei (BTH), Yangtze River Delta (YRD), and Pearl River Delta (PRD) urban agglomerations. CS = carbon storage; FP = food production; WY = water yield; PR = $PM_{2.5}$ removal; NR = nitrogen retention; SR = soil retention; HQ = habitat quality; RS = recreational opportunity. **(c)** The "d_{mr}" for multiple ESs in BTH, YRD, and PRD urban agglomerations.

Limitations and future perspectives

Although the InVEST models contain uncertainties and do not fully reflect the actual indicator values (Daneshi et al. 2021; Pickard et al. 2017), previous studies have confirmed that they performed well in certain regions, which included urbanization areas similar to the ones in the

current study (Redhead et al. 2016; Sun et al. 2018). Thus, the results of this study in the three urban agglomerations are relatively reliable. The models have been applied with multiple scales and have proven effective (Bagstad et al. 2018; Grafius et al. 2016; Nelson et al. 2009). Therefore, they could be used in the current study to explore the scaling relations and overall trends and changes of ESs. However, uncertainties still existed in the identification of scaling relationships for LULC and ESs. For example, the predictable scaling relationships for some ES indicators can be characterized by either the power law or the exponential function. The fitting functions were determined solely based on significance (P values) and determination coefficient (R^2) values. Future research should increase the sampled database of urban agglomerations and validate the scaling relations we proposed in this study. This will help in choosing more universal and reasonable regression models and in analyzing the underlying biophysical mechanisms behind them. Besides, previous research mainly focused on exploring how the natural and socio-economic attributes changed with different city scale (where population was usually used as the proxy indicator) (Bettencourt and Lobo 2016; Zhao et al. 2018a). These studies often adopted power law functions to express the relationships between city attributes and scales (Bettencourt 2013; Bettencourt et al. 2010; Wu 2004). In the future, we can compare the fitting curves derived from the scaling relations of the city scale indicator (e.g., population) or the spatial extent, to further understand the scale dependence of urban landscape patterns and ecological processes. In addition, we selected three highly developed national-level urban agglomerations in China to reflect the scaling relations of multiple LULC types and ESs. Previous study proved that the scaling relations of developed land in other six world metropolitan regions were closely resembled those of Beijing, Shanghai, and Guangzhou (Ma et al. 2019). In the future study, it still needs to be demonstrated whether the scaling relations of different LULC types and ESs would hold in urban agglomerations with other development levels in China or other countries.

Conclusions

Exploring how LULC and ES patterns change spatially across multiple scales is helpful for promoting urban landscape sustainability. Based on LULC maps and ES assessment results, this study used the scalogram forms to explore how different LULC types and ES indicators respond to changing spatial extents in the three largest urban agglomerations of China. The results revealed that different LULC mainly exhibited three types of scaling relations, linear, exponential, and sigmoidal relationships, among which developed land and cropland were the most predictable. LULC types at the city proper level were more predictable than the metropolitan and urban agglomeration levels. Most of the ES indicators increased when the spatial extent increased, but their scaling relations varied; provisioning services were the most predictable, while soil retention was unpredictable. The ESs predominantly presented two types of scaling functions, among which power law expressed ES patterns mainly at the lower levels while the exponential relationships were applicable to the higher levels. Among the three urban agglomerations, BTH performed the

best, while YRD performed the worst in the predictability of the ES spatial scaling. Since the scaling relations of ESs were deeply affected by the LULC patterns, implementing land use composition and configuring optimization strategies are conducive to ecological conservation planning, especially in the city proper. The scaling relations of ESs can provide a scientific basis for the boundary determination of urban land use management.

Acknowledgements

This work was supported by the National Natural Science Foundation of China [Grant No. 41901227 and U1901601], the Open Foundation of the State Key Laboratory of Urban and Regional Ecology of China [Grant No. SKLURE2020-2-1], and the Fundamental Research Funds for Central Non-profit Scientific Institution [Grant No. 1610132021001].

Declarations

Conflict of interest The authors declare that they have no conflict of interest.

References

Arcaute E, Hatna E, Ferguson P, Youn H, Johansson A, Batty M (2015) Constructing cities, deconstructing scaling laws. J R Soc Interface 12(102): 20140745

Bagstad KJ, Cohen E, Ancona ZH, McNulty SG, Sun G (2018) The sensitivity of ecosystem service models to choices of input data and spatial resolution. Appl Geogr 93: 25–36

Batty M (2008) The size, scale, and shape of cities. Science 319(5864): 769–771

Baumeister CF, Baumeister T, Plieninger T, Schraml U (2020) Exploring cultural ecosystem service hotspots: Linking multiple urban forest features with public participation mapping data. Urban For Urban Gree 48: 126561

Benra F, Frutos AD, Gaglio M, Álvarez-Garretón C, Felipe-Lucia M, Bonn A (2021) Mapping water ecosystem services: Evaluating InVEST model predictions in data scarce regions. Environ Modell Softw 3: 104982

Bettencourt LM (2013) The origins of scaling in cities. Science 340(6139): 1438–1441

Bettencourt LM, Lobo J (2016) Urban scaling in Europe. J R Soc Interface 13(116): 20160005

Bettencourt LM, Lobo J, Helbing D, Kühnert C, West GB (2007) Growth, innovation, scaling, and the pace of life in cities. Proc Natl Acad Sci USA 104(17): 7301–7306

Bettencourt LM, Lobo J, Strumsky D, West GB (2010) Urban scaling and its deviations: revealing the structure of wealth, innovation and crime across cities. PLoS One 5: e13541

Bian H, Gao J, Wu J, Sun X, Du Y (2020) Hierarchical analysis of landscape urbanization and its impacts on regional sustainability: A case study of the Yangtze River Economic Belt of China.

611 J Clean Prod 279: 123267
612 Bolliger J, Bättig MB, Gallati J, Kläy A, Stauffacher M, Kienast F (2011) Landscape
613 multifunctionality: a powerful concept to identify effects of environmental change. Reg
614 Environ Change 11: 203–206
615 Leitão AB, Ahern J (2002) Applying landscape ecological concepts and metrics in sustainable
616 landscape planning. Landsc Urban Plan 59:65–93
617 Brock WA (1999) Scaling in economics: a reader's guide. Ind Corp Change 8(3): 409–446
618 Brunet L, Tuomisaari J, Lavorel S, Crouzat E, Bierry A, Peltola T, Arpin I (2018) Actionable
619 knowledge for land use planning: Making ecosystem services operational. Land Use Policy
620 72: 27–34
621 Chen G, Li X, Liu X, Chen Y, Liang X, Leng J, Xu X, Liao W, Qiu Y, Wu Q, Huang K (2020)
622 Global projections of future urban land expansion under shared socioeconomic pathways. Nat
623 Commun 11: 1–12
624 Chen W, Yenneti K, We YD, Yuan F, Wu JW, Gao JL (2019) Polycentricity in the Yangtze River
625 Delta Urban Agglomeration (YRDUA): More Cohesion or More Disparities? Sustainability
626 11: 3106
627 Daneshi A, Brouwer R, Najafinejad A, Panahi M, Zarandian A, Maghsood FF (2021) Modelling
628 the impacts of climate and land use change on water security in a semi-arid forested
629 watershed using InVEST. J Hydrol 593: 125621
630 D'Amour C, Reitsma F, Baiocchi G, Barthel S, Güneralp B, Erb K, Haberl H, Creutzig F, Seto KC
631 (2016) Future urban land expansion and implications for global croplands. Proc Natl Acad
632 Sci USA 114 (34): 8939–8944
633 Department of Urban Surveys of National Bureau of Statistics of China (DUSNB) (2018) China
634 city statistics yearbook 2019. China Statistics Press, Beijing (in Chinese)
635 Du S, Wang Q, Guo L (2014) Spatially varying relationships between land-cover change and
636 driving factors at multiple sampling scales. J Environ Manage 137: 101–110
637 Du Y, Sun T, Peng J, Fang K, Liu Y, Yang Y, Wang Y (2018) Direct and spillover effects of
638 urbanization on $PM_{2.5}$ concentrations in China's top three urban agglomerations. J Clean Prod
639 190: 72–83
640 Fang C, Yu D (2017) Urban agglomeration: An evolving concept of an emerging phenomenon.
641 Landscape Urban Plan 162: 126–136
642 Fisher JI, Hurtt GC, Thomas RQ, Chambers JQ (2008) Clustered disturbances lead to bias in
643 large-scale estimates based on forest sample plots. Ecol Lett 11: 554–563
644 Forgione HM, Pregitzer CC, Charlop-Powers S, Gunther B (2016) Advancing urban ecosystem
645 governance in New York City: Shifting towards a unified perspective for conservation
646 management. Environ Sci Pol 62: 127–132
647 Frazier AE (2016) Surface metrics: scaling relationships and downscaling behavior. Landscape
648 Ecol 31: 351–363.

649 Fuller RA, Gaston KJ (2009) The scaling of green space coverage in European cities. Biol Lett
650 5(3): 352–355
651 Gao J, Yu ZW, Wang LC, Vejre H (2019) Suitability of regional development based on ecosystem
652 service benefits and losses: A case study of the Yangtze River Delta urban agglomeration,
653 China. Ecol Indic 107: 105579
654 Goldstein JH, Caldarone G, Duarte TK, Ennaanay D, Hannahs N, Mendoza G, Polasky S, Wolny
655 S, Daily GC (2012) Integrating ecosystem-service tradeoffs into land-use decisions. P Natl
656 Acad Sci USA 109(19): 7565–7570
657 Grafius DR, Corstanje R, Warren PH, Evans KL, Hancock S, Harris JA (2016) The impact of land
658 use/land cover scale on modelling urban ecosystem services. Landscape Ecol 31: 1509–1522
659 Gu C (2019) Urbanization: Processes and driving forces. Sci China Earth Sci 62(9): 1351–1360
660 Hamel P, Chaplin-Kramer R, Sim S, Mueller C (2015) A new approach to modeling the sediment
661 retention service (InVEST 3.0): Case study of the Cape Fear catchment, North Carolina, USA.
662 Sci Total Environ 524–525: 166–177
663 Hasan SS, Zhen L, Miah MG, Ahamed T, Samie A (2020) Impact of land use change on ecosystem
664 services: A review. Environ Dev 34: 100527
665 Hein L, van Koppen K, de Groot RS, van Ierland EC (2006) Spatial scales, stakeholders and the
666 valuation of ecosystem services. Ecol Econ 57: 209–228
667 Hu M, Li Z, Wang Y, Jiao M, Li M, Xia B (2019) Spatio-temporal changes in ecosystem service
668 value in response to land-use/cover changes in the Pearl River Delta. Resour Conserv Recy
669 149: 106–114
670 Jomnonkwao S, Uttra S, Ratanavaraha V (2020) Forecasting road traffic deaths in Thailand:
671 applications of Time-Series, curve estimation, multiple linear regression, and path analysis
672 models. Sustainability 12(1): 395
673 Kedron PJ, Frazier AE, Ovando-Montejo GA, Wang J (2018) Surface metrics for landscape
674 ecology: a comparison of landscape models across ecoregions and scales. Landscape Ecol 33:
675 1489–1504.
676 Korkanç SY, Dorum G (2019) The nutrient and carbon losses of soils from different land cover
677 systems under simulated rainfall conditions. CATENA 172: 203–211
678 Kuang B, Lu X, Han J, Fan X, Zuo J (2020) How urbanization influence urban land consumption
679 intensity: Evidence from China. Habitat Int 100: 102103
680 Kuang W (2020a) 70 years of urban expansion across China: trajectory, pattern, and national
681 policies. Sci Bull 65: 1970–1974
682 Kuang W (2020b) National urban land-use/cover change since the beginning of the 21st century
683 and its policy implications in China. Land Use Policy 97: 104747
684 Lan T, Shao G, Xu Z, Tang L, Sun L (2021) Measuring urban compactness based on functional
685 characterization and human activity intensity by integrating multiple geospatial data sources.
686 Ecol Indic 121: 107177

687 Lan X, Tang H, Liang H (2017) A theoretical framework for researching cultural ecosystem
688 service flows in urban agglomerations. Ecosyst Serv 28: 95–104
689 Lavorel S, Rey P, Grigulis K, Zawada M, Byczek C (2020) Interactions between outdoor
690 recreation and iconic terrestrial vertebrates in two French alpine national parks. Ecosyst Serv
691 45: 101155
692 Lawler J, Lewis D, Nelson E, Plantinga A, Polasky S, Withey J, Helmers D, Martinuzzi S,
693 Pennington D, Radeloff V (2014) Projected land-use change impacts on ecosystem services
694 in the United States. Proc Natl Acad Sci USA 111(20): 7492–7497
695 Lei J, Wang S, Wu J, Wang J, Xiong X (2021) Land-use configuration has significant impacts on
696 water-related ecosystem services. Ecol Eng 160: 106133
697 Li C, Li J, Wu J (2013) Quantifying the speed, growth modes, and landscape pattern changes of
698 urbanization: a hierarchical patch dynamics approach. Landscape Ecol 28(10): 1875–1888
699 Li H, Peng J, Liu Y, Hu Y (2017) Urbanization impact on landscape patterns in Beijing City, China:
700 A spatial heterogeneity perspective. Ecol Indic 82: 50–60
701 Li W, Hai X, Han L, Mao J, Tian M (2020) Does urbanization intensify regional water scarcity?
702 Evidence and implications from a megaregion of China. J Clean Prod 244: 118592
703 Li F, Zhou T (2019) Effects of urban form on air quality in China: An analysis based on the spatial
704 autoregressive model. Cities 89: 130–140
705 Lin JY, Li X (2019) Large-scale ecological red line planning in urban agglomerations using a
706 semi-automatic intelligent zoning method. Sustain Cities Soc 46: 101410
707 Liu L, Xu X, Chen X (2015) Assessing the impact of urban expansion on potential crop yield in
708 China during 1990–2010. Food Sec 7: 33–43
709 Liu W, Zhan J, Zhao F, Yan H, Zhang F, Wei X (2019) Impacts of urbanization-induced land-use
710 changes on ecosystem services: A case study of the Pearl River Delta Metropolitan Region,
711 China. Ecol Indic 98: 228–238
712 Liu Y, Zhang X, Kong X, Wang R, Chen L (2018) Identifying the relationship between urban land
713 expansion and human activities in the Yangtze River Economic Belt, China. Appl Geogr 94:
714 163–177
715 Liu Y, Zhang X, Pan X, Ma X, Tang M (2020) The spatial integration and coordinated industrial
716 development of urban agglomerations in the Yangtze River Economic Belt, China. Cities 104:
717 102801
718 Lobo J, Bettencourt LM, Smith ME, Ortman S (2020) Settlement scaling theory: Bridging the
719 study of ancient and contemporary urban systems. Urban Stud 57(4): 731–747
720 Lu D, Mao W, Yang D, Zhao J, Xu J (2018) Effects of land use and landscape pattern on $PM_{2.5}$ in
721 Yangtze River Delta, China. Atmos Pollut Res 9(4): 705–713
722 Luo Q, Zhang X, Li Z, Yang M, Lin Y (2018) The effects of China's Ecological Control Line
723 policy on ecosystem services: The case of Wuhan City. Ecol Indic 93: 292–301
724 Luo Q, Zhou J, Li Z, Yu B (2020) Spatial differences of ecosystem services and their driving

725 factors: A comparation analysis among three urban agglomerations in China's Yangtze River
726 Economic Belt. Sci Total Environ 725: 138452
727 Ma Q, He C, Wu J (2016) Behind the rapid expansion of urban impervious surfaces in China:
728 Major influencing factors revealed by a hierarchical multiscale analysis. Land Use Policy, 59,
729 434–445
730 Ma Q, Wu J, He C (2016b). A hierarchical analysis of the relationship between urban impervious
731 surfaces and land surface temperatures: spatial scale dependence, temporal variations, and
732 bioclimatic modulation. Landscape Ecol 31(5): 1139–1153
733 Ma Q, Wu J, He C, Hu G (2019) Reprint of "Spatial scaling of urban impervious surfaces across
734 evolving landscapes: From cities to urban regions". Landscape Urban Plan 187: 132–144
735 Massada AB, Radeloff VC (2010) Two multi-scale contextual approaches for mapping spatial
736 pattern. Landscape Ecol 25: 711–725
737 Millennium Ecosystem Assessment (2005) Ecosystems and Human Well-Being: Synthesis. Island
738 Press, Washington, DC
739 Mitchell MGE, Bennett EM, Gonzalez A (2015) Strong and nonlinear effects of fragmentation on
740 ecosystem service provision at multiple scales. Environ Res Lett 10: 094014
741 Momblanch A, Connor JD, Crossman ND, Paredes-Arquiola J, Andreu J (2016) Using ecosystem
742 services to represent the environment in hydro-economic models. J Hydrol 522: 95–109
743 Nelson E, Mendoza G, Regetz J, Polasky S, Tallis H, Cameron D, Chan KMA, Daily GC,
744 Goldstein J, Kareiva PM, Lonsdorf E, Naidoo R, Ricketts TH, Shaw M (2009) Modeling
745 multiple ecosystem services, biodiversity conservation, commodity production, and tradeoffs
746 at landscape scales. Front Ecol Environ 7(1): 4–11
747 Newman MEJ (2005) Power laws, Pareto distributions and Zipf's law. Contemp Phys 46: 323–351
748 Nikodinoska N, Paletto A, Pastorella F, Granvik M, Franzese PP (2018) Assessing, valuing and
749 mapping ecosystem services at city level: The case of Uppsala (Sweden). Ecol Model 121:
750 107028
751 Normile D (2016) China rethinks cities. Science 352(6288): 916–918
752 O'Neill RV, Deangelis DL, Waide JB, Allen GE (1986) A hierarchical concept of ecosystems.
753 Princeton University Press, New Jersey
754 Patra S, Sahoo S, Mishra P, Mahapatra SC (2018) Impacts of urbanization on land use/cover
755 changes and its probable implications on local climate and groundwater level. J Urban Manag
756 7(2): 70–84
757 Peng J, Liu Y, Liu Z, Yang Y (2017) Mapping spatial non-stationarity of human-natural factors
758 associated with agricultural landscape multifunctionality in Beijing–Tianjin–Hebei region,
759 China. Agric Ecosyst Environ 246: 221–233
760 Pickard BR, Berkel DV, Petrasova A, Meentemeyer RK (2017) Forecasts of urbanization
761 scenarios reveal trade-offs between landscape change and ecosystem services. Landscape
762 Ecol 32: 617–634

763 Poku-Boansi M (2012) Contextualizing urban growth, urbanisation and travel behaviour in
764 Ghanaian cities. Cities 110: 103083
765 Redhead JW, Stratford C, Sharps K, Jones L, Ziv G, Clarke D, Oliver TH, Bullock JM (2016)
766 Empirical validation of the InVEST water yield ecosystem service model at a national scale.
767 Sci Total Environ 569–570: 1418–1426
768 Ribeiro FL, Meirelles J, Netto VM, Neto CR, Baronchelli A (2020) On the relation between
769 transversal and longitudinal scaling in cities. PLoS One 15(5): 1–20
770 Rieb JT, Bennett EM (2020) Landscape structure as a mediator of ecosystem service interactions.
771 Landscape Ecol 35: 2863–2880
772 Robinson DT, Brown DG, Currie WS (2009) Modelling carbon storage in highly fragmented and
773 human-dominated landscapes: Linking land-cover patterns and ecosystem models. Ecol
774 Modell 220(9): 1325–1338
775 Rodríguez-Caballero E, Cantón Y, Chamizo S, Lázaro R, Escudero A (2013) Soil loss and runoff
776 in semiarid ecosystems: a complex interaction between biological soil crusts,
777 micro-topography, and hydrological drivers. Ecosystems 16: 529–546
778 Seto KC, Reenberg A, Boone CG, Fragkias M, Haase D, Langanke T, Marcotullio P, Munroe DK,
779 Olah B, Simon D (2012) Urban land teleconnections and sustainability. Proc Natl Acad Sci
780 USA 109(20): 7687–7692
781 Smith P, Adams J, Beerling DJ, Beringer T, Calvin KV, Fuss S, Griscom B, Hagemann N,
782 Kammann C, Kraxner F, Minx JC, Popp A, Renforth P, Luis J, Vicente V, Keesstra S (2019)
783 Land-Management options for greenhouse gas removal and their impacts on ecosystem
784 services and the sustainable development goals. Annu Rev Environ Resour 44: 255–286
785 Sharp R, Douglass J, Wolny S, Arkema K, Bernhardt J, Bierbower W, Chaumont N, Denu D,
786 Fisher D, Glowinski K, Griffin R, Guannel G, Guerry A, Johnson J, Hamel P, Kennedy C,
787 Kim CK, Lacayo M, Lonsdorf E, Mandle L, Rogers L, Silver J, Toft J, Verutes G, Vogl AL,
788 Wood S, Wyatt K (2020) InVEST 3.8.9.post9+ug.ga009fc0 User's Guide. The Natural
789 Capital Project, Stanford University, University of Minnesota, The Nature Conservancy, and
790 World Wildlife Fund
791 Shen J, Li S, Liang Z, Liu L, Li D, Wu S (2020) Exploring the heterogeneity and nonlinearity of
792 trade-offs and synergies among ecosystem services bundles in the Beijing-Tianjin-Hebei
793 urban agglomeration. Ecosyst Serv 43: 101103
794 Shoemaker DA, BenDor TK, Meentemeyer RK (2019) Anticipating trade-offs between urban
795 patterns and ecosystem service production: Scenario analyses of sprawl alternatives for a
796 rapidly urbanizing region. Comput Environ Urban 74: 114–125
797 Spence AJ (2009) Scaling in biology. Curr Biol CB 19: R57–R61
798 Stokes EC, Seto KC (2019) Characterizing and measuring urban landscapes for sustainability.
799 Environ Res Lett 14: 045002
800 Sun W, Shao Q, Liu J, Zhai J (2014) Assessing the effects of land use and topography on soil

erosion on the Loess Plateau in China. CATENA 121: 151–163
Sun X, Lu ZM, Li F, Crittenden JC (2018) Analyzing spatio-temporal changes and trade-offs to support the supply of multiple ecosystem services in Beijing, China. Ecol Indic 94: 117–129
Sun X, Tan X, Chen K, Song S, Zhu X, Hou D (2020) Quantifying landscape-metrics impacts on urban green-spaces and water-bodies cooling effect: The study of Nanjing, China. Urban For Urban Gree 55: 126838
Swenson JJ, Franklin J (2000) The effects of future urban development on habitat fragmentation in the Santa Monica Mountains. Landscape Ecol 15: 713–730
Tao Y, Zhang Z, Ou WX, Guo J, Pueppke SG (2020) How does urban form influence $PM_{2.5}$ concentrations: Insights from 350 different-sized cities in the rapidly urbanizing Yangtze River Delta region of China, 1998–2015. Cities 98: 102581
Verburg PH, de Groot WT, Veldkamp AJ (2003) Methodology for Multi-Scale Land-Use Change Modelling: Concepts and Challenges. Global Environmental Change and Land Use. Springer, Dordrecht. https://doi.org/10.1007/978-94-017-0335-2_2
Viglizzo EF, Paruelo JM, Laterra P, Jobbágy EG (2012) Ecosystem service evaluation to support land-use policy. Agr Ecosyst Environ 154: 78–84
Wang LZ, Omrani H, Zhao Z, Francomano D, Li K, Pijanowski B (2019) Analysis on urban densification dynamics and future modes in southeastern Wisconsin, USA. PLoS One 14(3): 0211964
Wang Z, Liang L, Sun Z, Wang X (2019b) Spatiotemporal differentiation and the factors influencing urbanization and ecological environment synergistic effects within the Beijing-Tianjin-Hebei urban agglomeration. J Environ Manage 243: 227–239
Wang Z, Zhang S, Peng Y, Wu C, Lv Y, Xiao K, Zhao J, Qian G (2020) Impact of rapid urbanization on the threshold effect in the relationship between impervious surfaces and water quality in shanghai, China. Environ Pollut 267: 115569
Wu J (1999) Hierarchy and scaling: extrapolating information along a scaling ladder. Can J Remote Sens 25(4): 367–380
Wu J (2004) Effects of changing scale on landscape pattern analysis: scaling relations. Landscape Ecol 19: 125–138
Wu J, David JL (2002) A spatially explicit hierarchical approach to modeling complex ecological systems: theory and applications. Ecol Model 153(1): 7–26
Wu J, Jenerette GD, Buyantuyev A, Redman CL (2011) Quantifying spatiotemporal patterns of urbanization: The case of the two fastest growing metropolitan regions in the United States. Ecol Complex 8(1): 1–8
Wu J, Li H (2006) Perspectives and methods of scaling. In Wu J, Jones B, Li H, Loucks OL (Eds.). Scaling and uncertainty analysis in ecology. Springer, Dordrecht, pp 17–44
Wu J, Shen WJ, Sun WZ, Tueller PT (2002) Empirical patterns of the effects of changing scale on landscape metrics. Landsc Ecol 17: 761–782

839 Wu R, Li Z, Wang S (2020) The varying driving forces of urban land expansion in China: Insights
840 from a spatial-temporal analysis. Sci Total Environ 8: 142591
841 Xie H, He Y, Xie X (2017) Exploring the factors influencing ecological land change for China's
842 Beijing–Tianjin–Hebei Region using big data. J Clean Prod 142: 677–687
843 Xing L, Zhu Y, Wang J (2021) Spatial spillover effects of urbanization on ecosystem services
844 value in Chinese cities. Ecol Indic 121: 107028
845 Xu C, Zhao S, Liu S (2020) Spatial scaling of multiple landscape features in the conterminous
846 United States. Landsc Ecol 35: 223–247
847 Xu Q, Dong Y, Yang R (2018) Influence of land urbanization on carbon sequestration of urban
848 vegetation: A temporal cooperativity analysis in Guangzhou as an example. Sci Total Environ
849 635: 26–34
850 Yang D, Liu W, Tang L, Chen L, Li X, Xu X (2019) Estimation of water provision service for
851 monsoon catchments of South China: Applicability of the InVEST model. Landscape Urban
852 Plan 182: 133–143
853 Yang J, Yang J, Luo X, Huang C (2019) Impacts by expansion of human settlements on nature
854 reserves in China. J Environ Manag 248: 109233
855 Yee SH, Paulukonis E, Simmons C, Russell M, Fulford R, Harwell L, Smith LM (2021) Projecting
856 effects of land use change on human well-being through changes in ecosystem services. Ecol
857 Modell 440: 109358
858 Yu J, Zhou K, Yang S (2019) Land use efficiency and influencing factors of urban agglomerations
859 in China. Land Use Policy 88: 104143
860 Zhang D, Huang Q, He C, Wu J (2017) Impacts of urban expansion on ecosystem services in the
861 Beijing-Tianjin-Hebei urban agglomeration, China: A scenario analysis based on the Shared
862 Socioeconomic Pathways. Resour Conserv Recycl 125: 115–130
863 Zhang Y, Hu Y, Zhuang D (2020a) A highly integrated, expansible, and comprehensive analytical
864 framework for urban ecological land: A case study in Guangzhou, China. J Clean Prod 268:
865 122360
866 Zhang P, Kohli D, Sun Q, Zhang Y, Liu S, Sun D (2020b) Remote sensing modeling of urban
867 density dynamics across 36 major cities in China: Fresh insights from hierarchical urbanized
868 space. Landscape Urban Plan 203: 103896
869 Zhang X, Zhong T, Wang K, Cheng Z (2009) Scaling of impervious surface area and vegetation as
870 indicators to urban land surface temperature using satellite data. Int J Remote Sens 30(4):
871 841–859
872 Zhao S, Liu S (2014) Scale criticality in estimating ecosystem carbon dynamics. Glob Change
873 Biol 20: 2240–2251
874 Zhao S, Liu S, Xu C, Yuan W, Sun Y, Yan W, Zhao M, Henebry GM, Fang J (2018a)
875 Contemporary Evolution and Scaling of 32 Major Cities in China. Ecol Appl 28(6): 1655–
876 1668

877 Zhou D, Tian Y, Jiang G (2018b) Spatio-temporal investigation of the interactive relationship
878 between urbanization and ecosystem services: Case study of the Jingjinji urban
879 agglomeration, China. Ecol Indic 95: 152–164
880 Zhou Y, Chen M, Tang Z, Mei Z (2021) Urbanization, land use change, and carbon emissions:
881 Quantitative assessments for city-level carbon emissions in Beijing-Tianjin-Hebei region.
882 Sustain Cities Soc 66: 102701

Figures

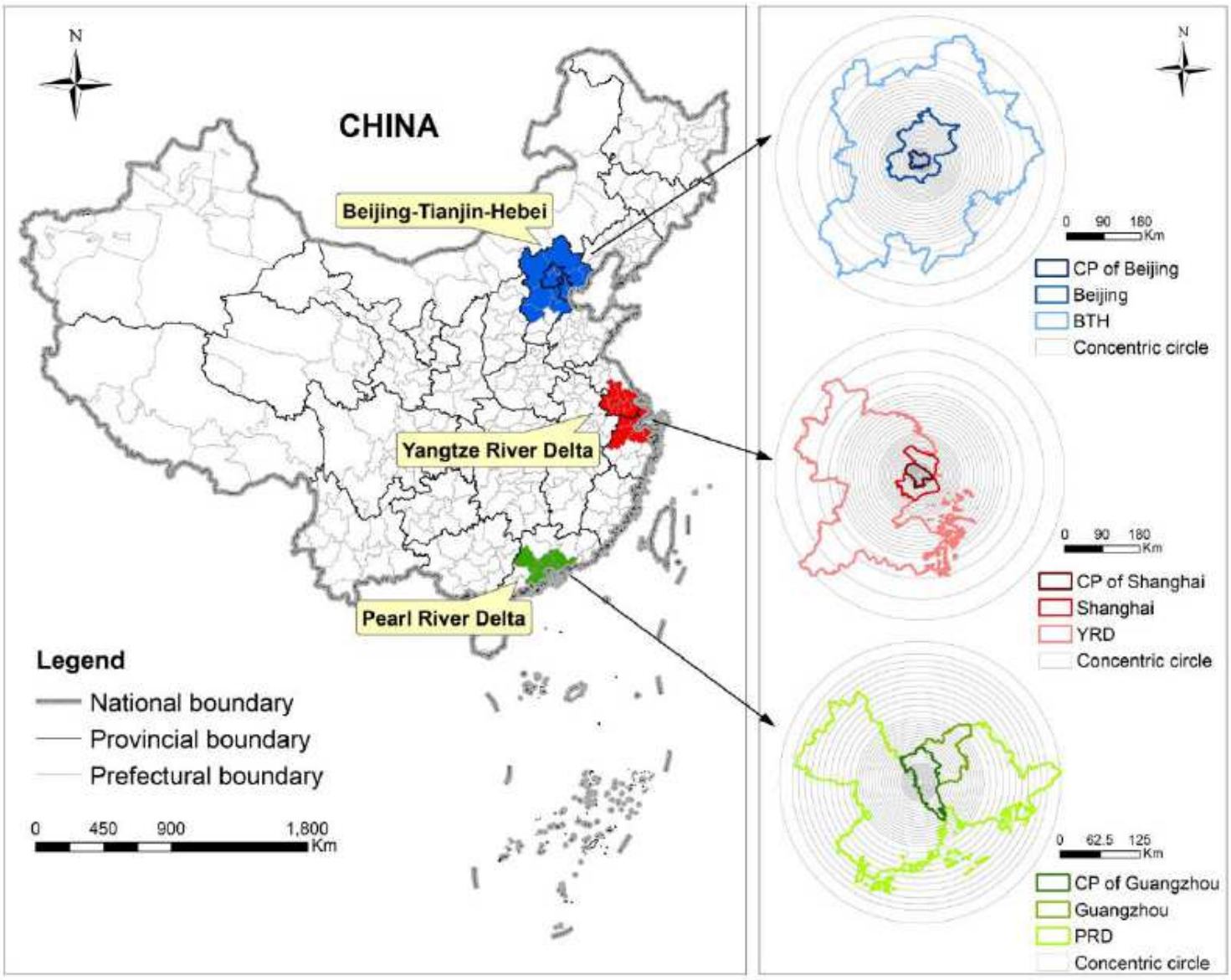

Figure 1

Location and administrative hierarchy of study areas. The concentric circle illustrations on the right represent the spatial extension of three urban agglomerations at the administrative hierarchy levels. The CP of Beijing/Shanghai/Guangzhou refer to the city proper of Beijing/Shanghai/Guangzhou; Beijing/Shanghai/Guangzhou refer to the Beijing/Shanghai/Guangzhou metropolitan region; BTH/YRD/PRD refer to the Beijing Tianjin Hebei/Yangtze River Delta/Pearl River Delta urban agglomeration. Note: The designations employed and the presentation of the material on this map do not imply the expression of any opinion whatsoever on the part of Research Square concerning the legal status of any country, territory, city or area or of its authorities, or concerning the delimitation of its frontiers or boundaries. This map has been provided by the authors.

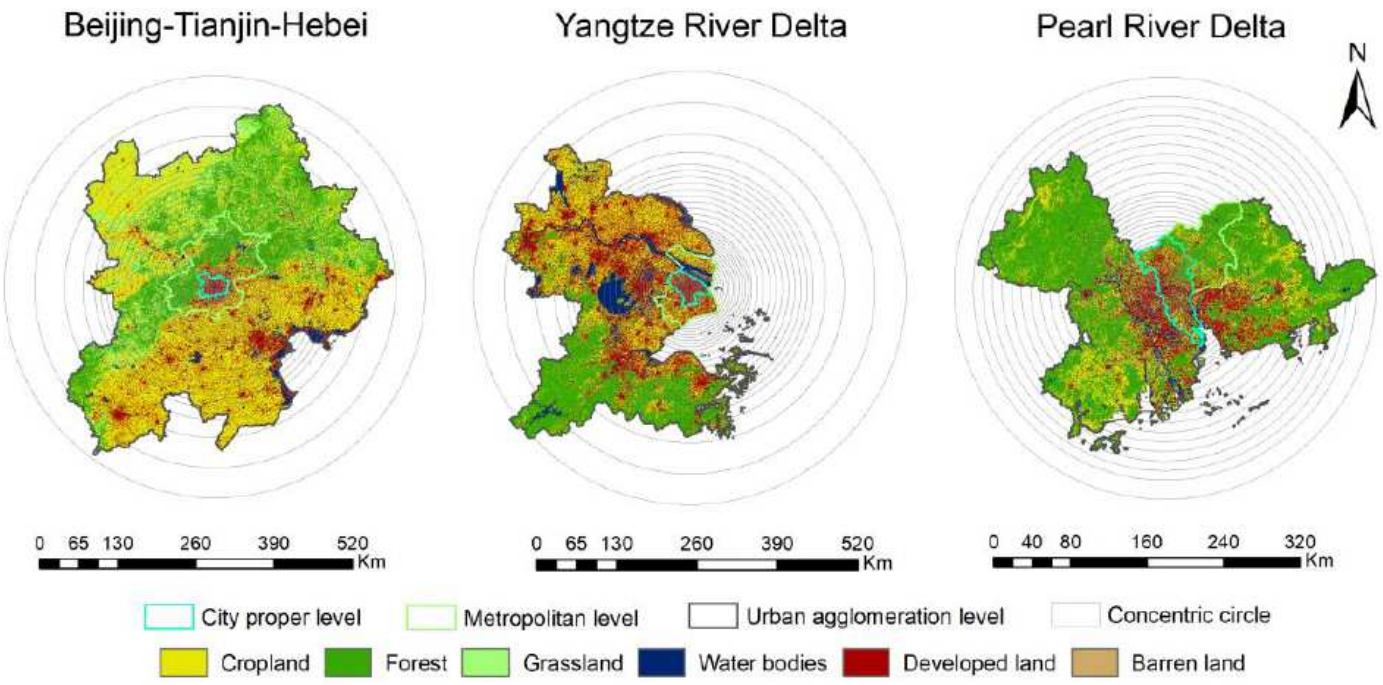

Figure 2

Spatial distributions of land use/land cover in 2018 for three urban agglomerations. The radii list of concentric circles is shown in Table 2. Note: The designations employed and the presentation of the material on this map do not imply the expression of any opinion whatsoever on the part of Research Square concerning the legal status of any country, territory, city or area or of its authorities, or concerning the delimitation of its frontiers or boundaries. This map has been provided by the authors.

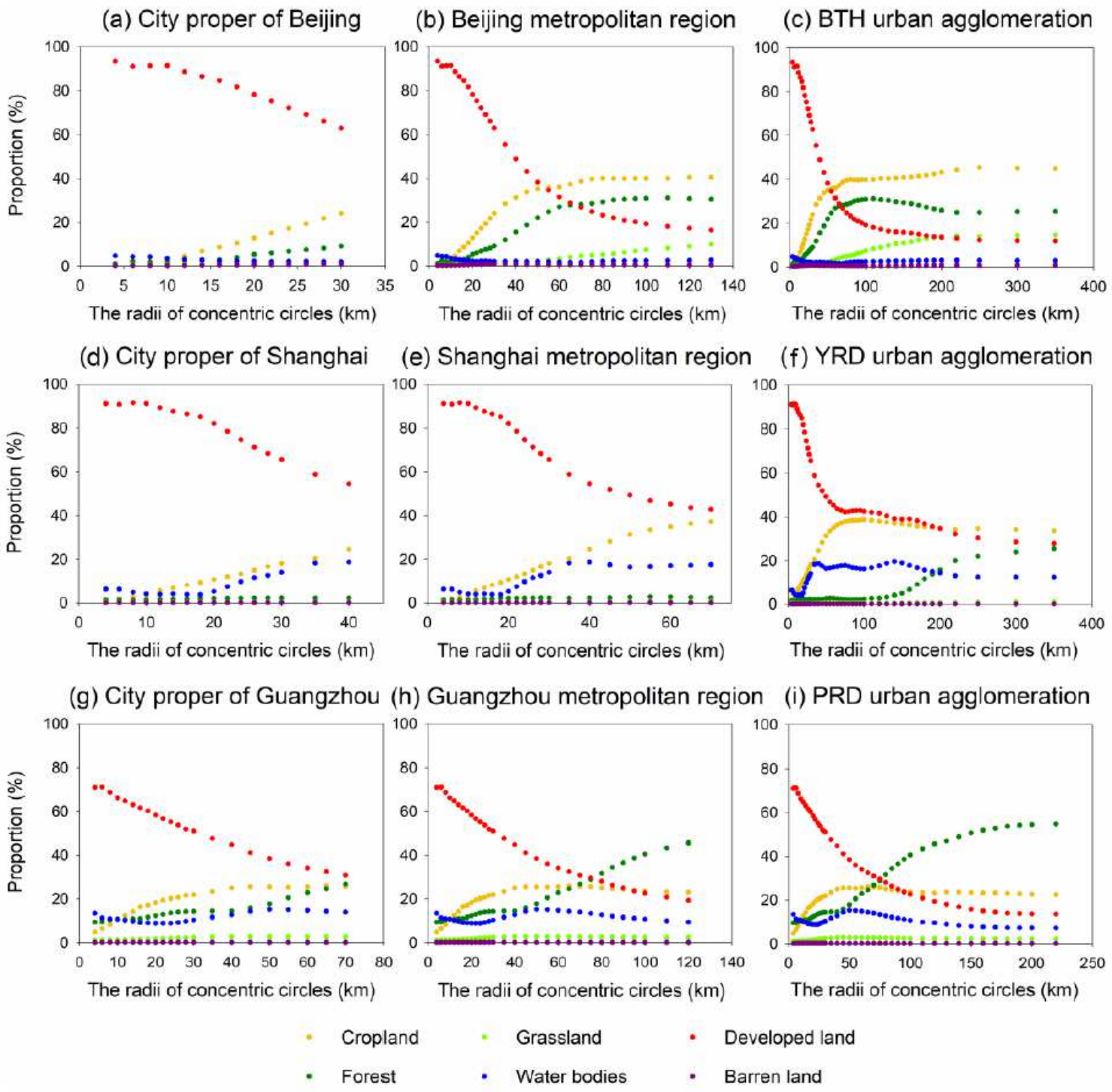

Figure 3

Scalograms of the proportion of different land use /land cover types with respect to increasing concentric circle radii in the three largest urban agglomerations of China (Beijing Tianjin Hebei (BTH), Yangtze River Delta (YRD), and Pearl River Delta (PRD)).

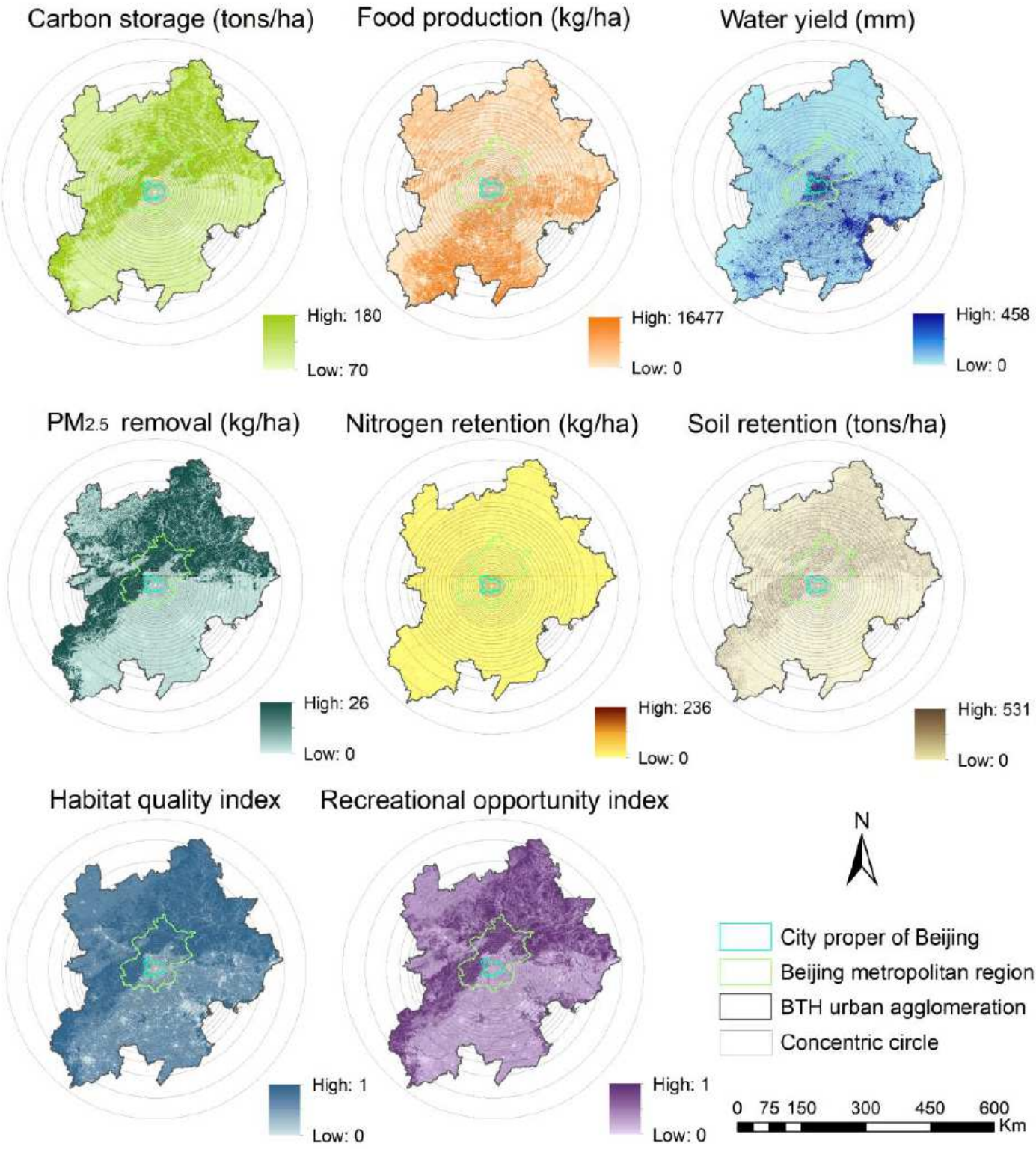

Figure 4

Spatial distributions of multiple ecosystem services in 2018 for Beijing Tianjin-Hebei (BTH) urban agglomeration. The radii list of concentric circles was shown in Table 2. Note: The designations employed and the presentation of the material on this map do not imply the expression of any opinion whatsoever on the part of Research Square concerning the legal status of any country, territory, city or

area or of its authorities, or concerning the delimitation of its frontiers or boundaries. This map has been provided by the authors.

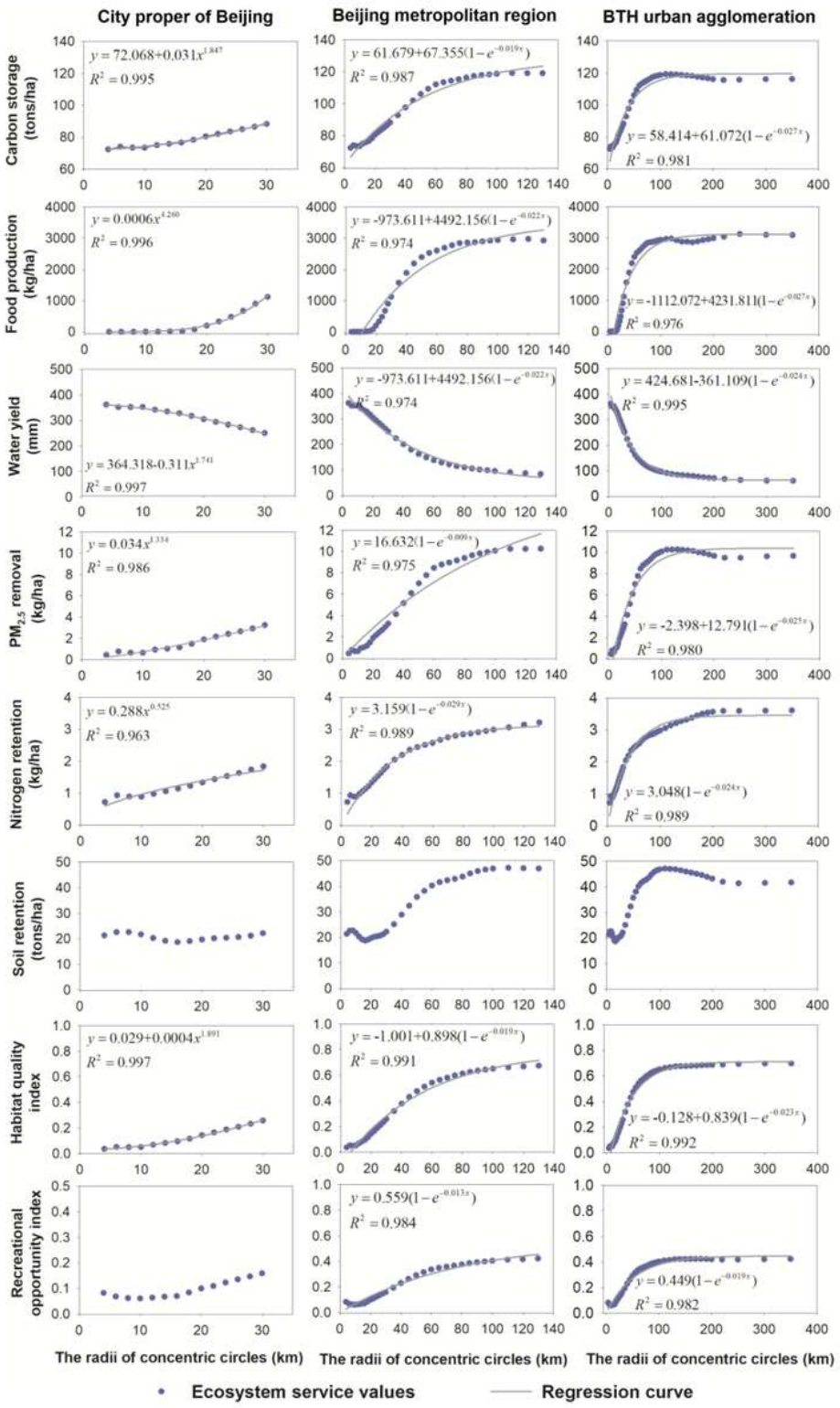

Figure 5

Scalograms of multiple ecosystem service indicators with respect to increasing concentric circle radii at various urban hierarchical levels: the city proper of Beijing, Beijing metropolitan region, and the Beijing Tianjin Hebei (BTH). F or all regression curves and equations, the 269 significance level P values < 0.001.

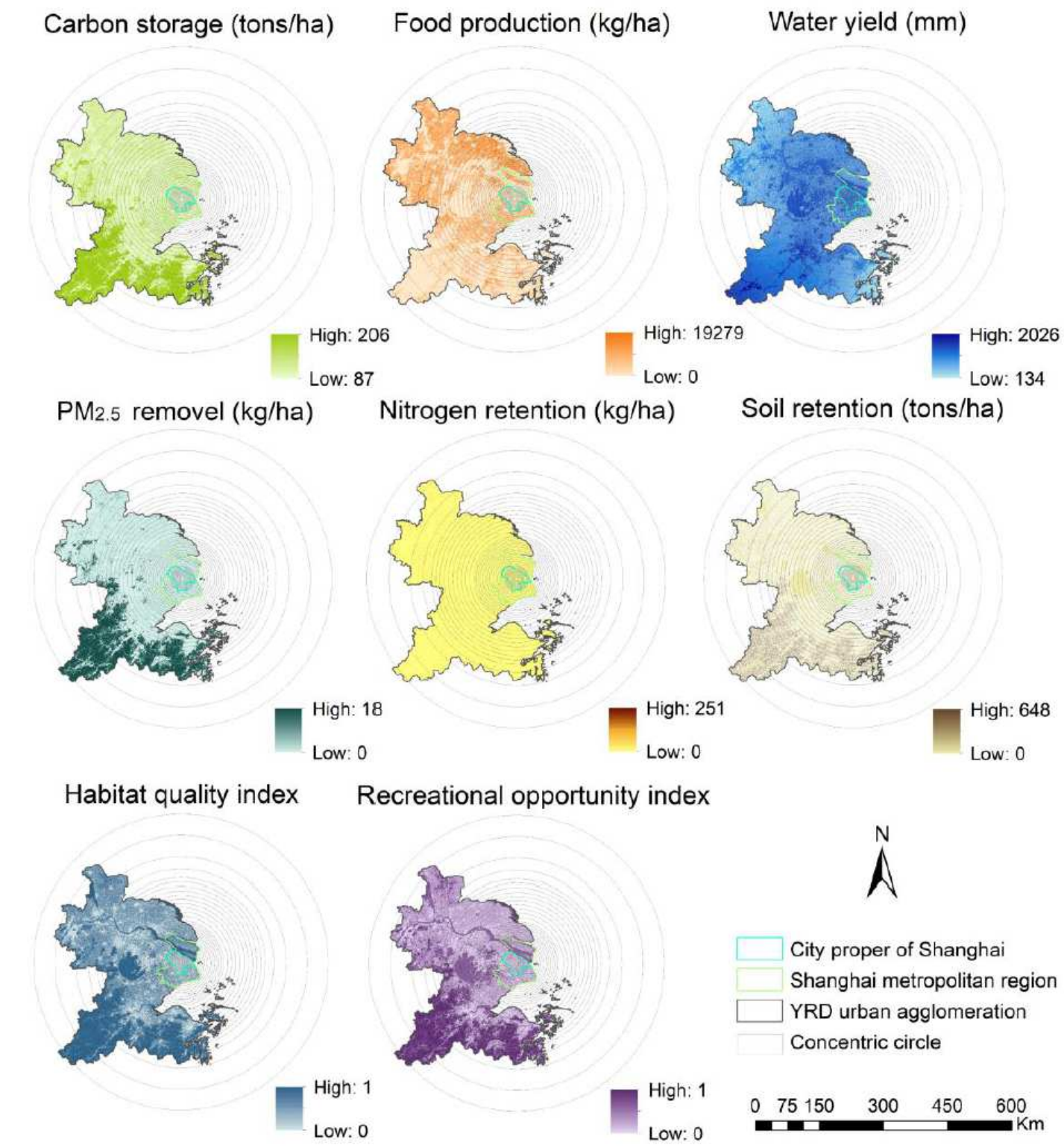

Figure 6

Spatial distributions of multiple ecosystem services in 2018 for Yangtze River Delta (YRD) urban agglomeration. The radii list of concentric circles was shown in Table 2. Note: The designations employed and the presentation of the material on this map do not imply the expression of any opinion whatsoever on the part of Research Square concerning the legal status of any country, territory, city or

area or of its authorities, or concerning the delimitation of its frontiers or boundaries. This map has been provided by the authors.

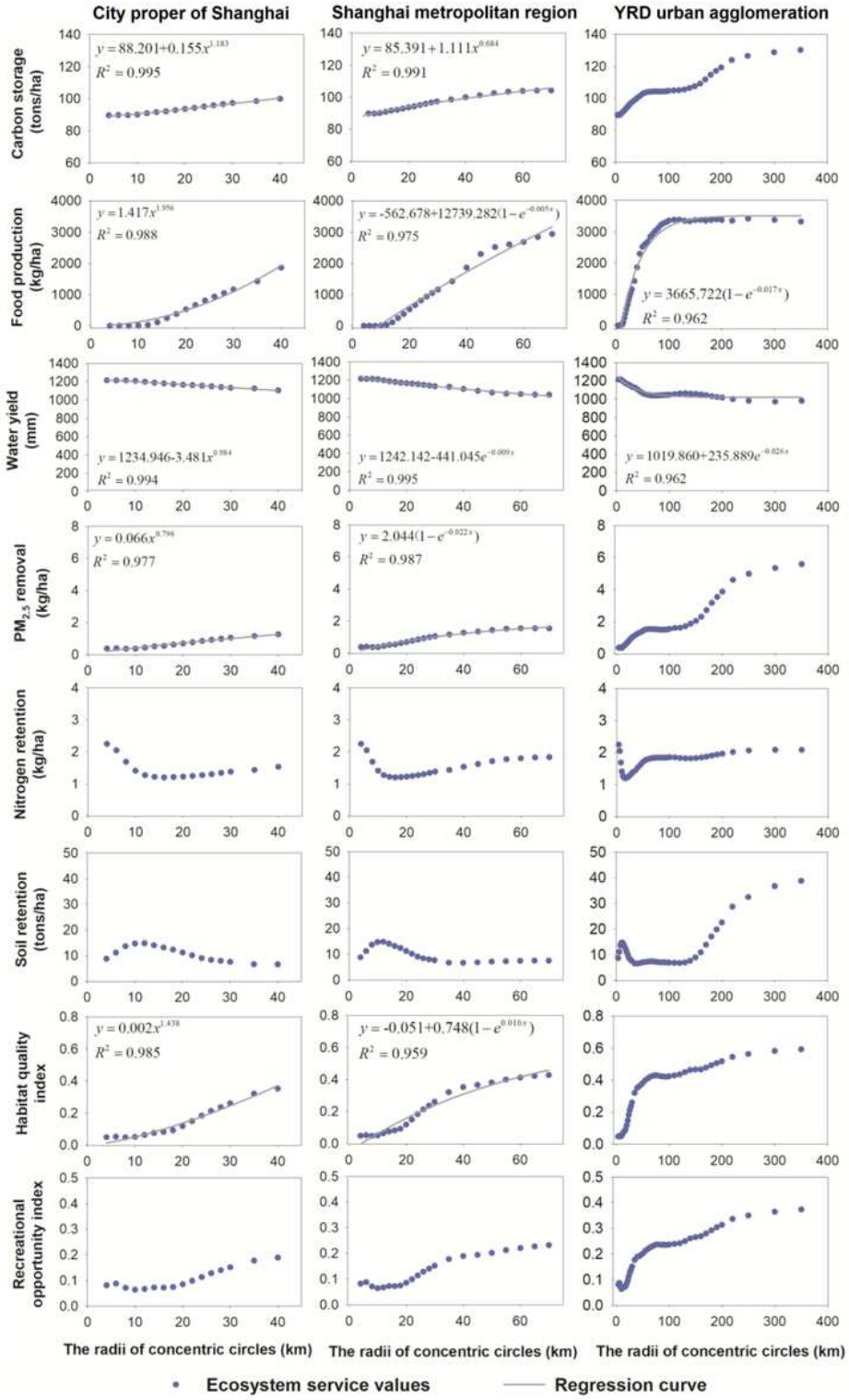

Figure 7

Scalograms of multiple ecosystem service indicators with respect to increasing concentric circle radii at various urban hierarchical levels: the city proper of Shanghai, Shanghai metropolitan region, and the

Yangtze River Delta (YRD). For all regression curves and equations, the significance level P values < 0.001.

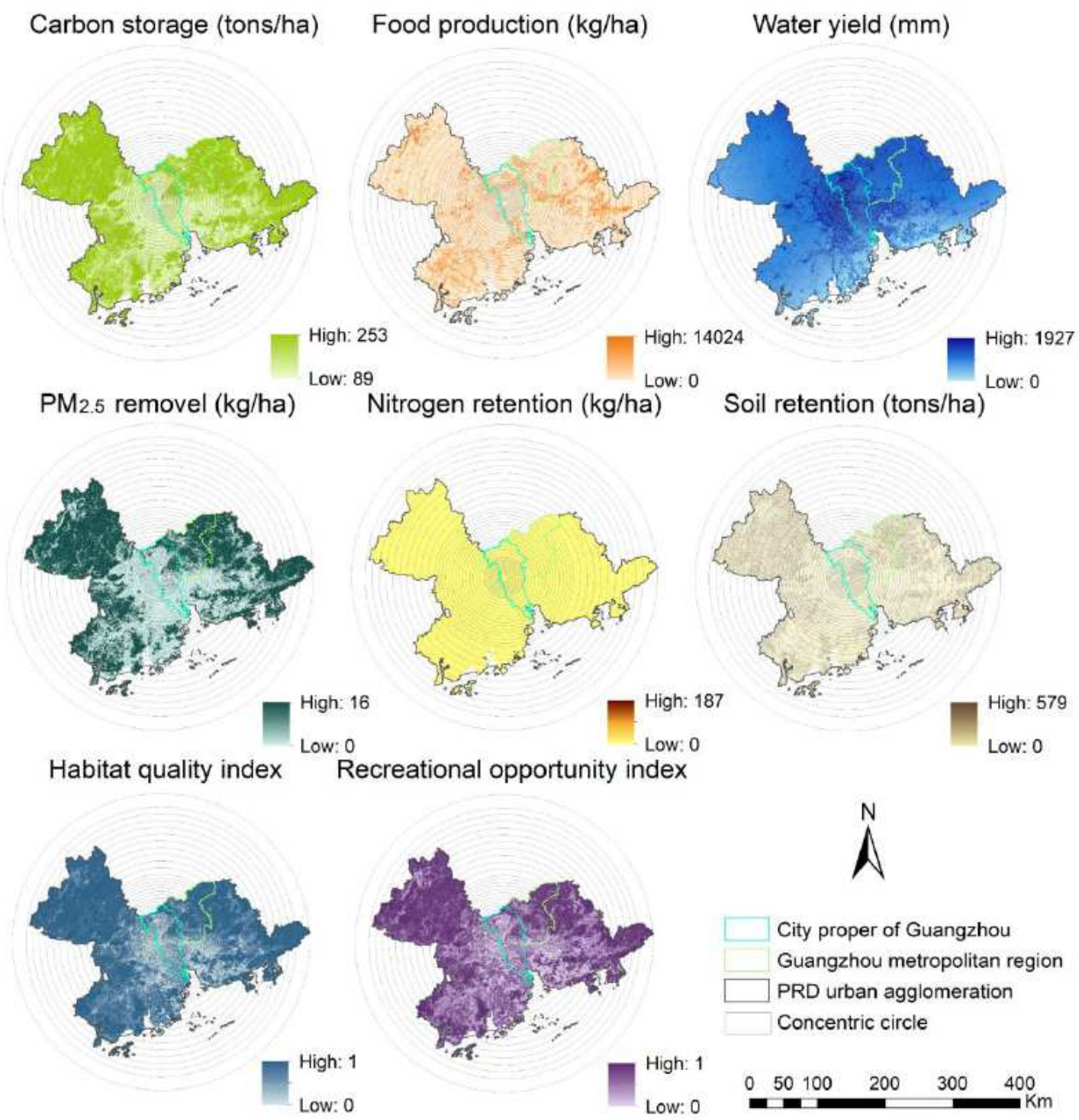

Figure 8

Spatial distributions of multiple ecosystem services in 2018 for Pearl River Delta (PRD) urban agglomeration. The radii list of concentric circles was shown in Table 2. Note: The designations employed and the presentation of the material on this map do not imply the expression of any opinion

whatsoever on the part of Research Square concerning the legal status of any country, territory, city or area or of its authorities, or concerning the delimitation of its frontiers or boundaries. This map has been provided by the authors.

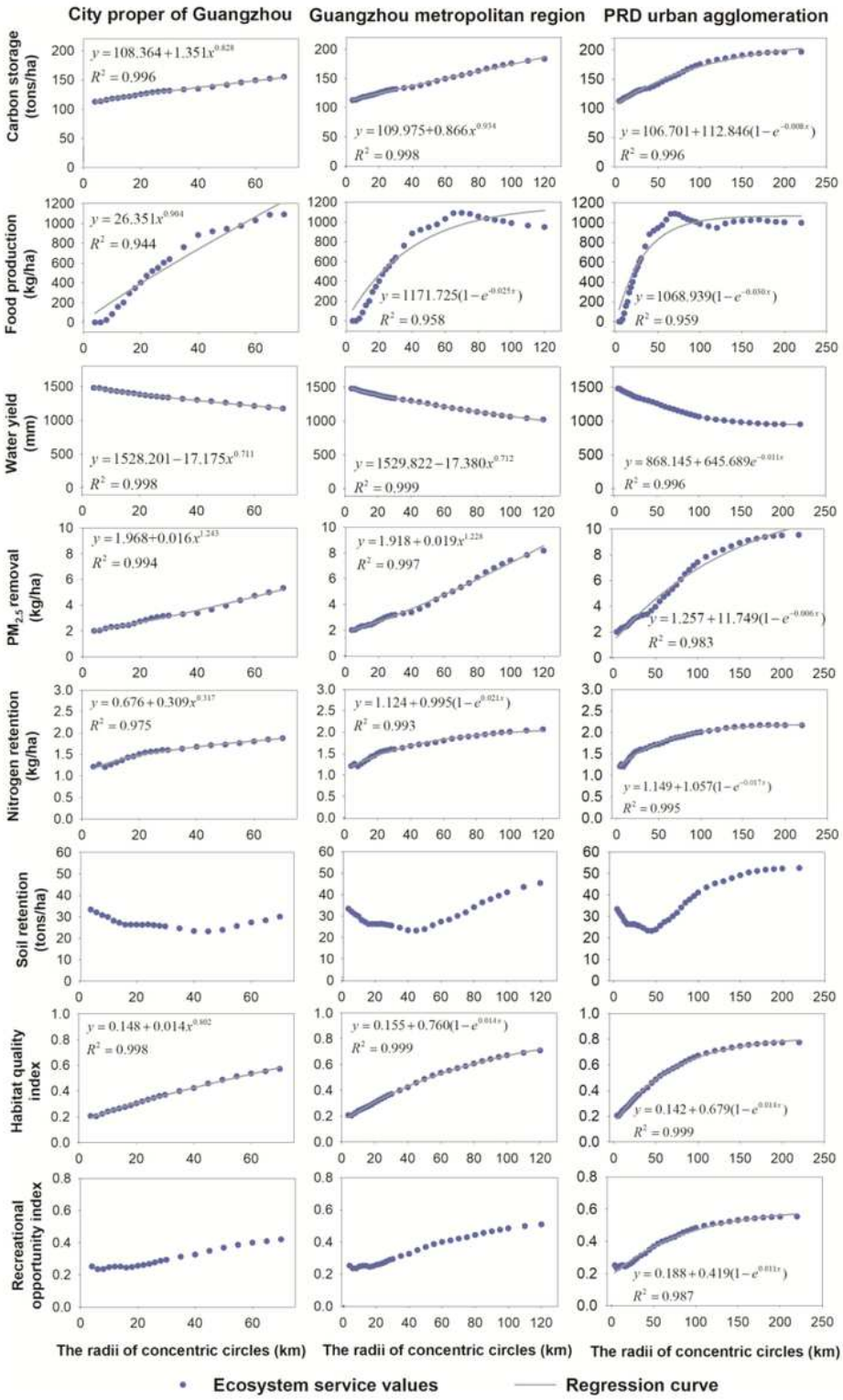

Figure 9

Scalograms of multiple ecosystem service indicators with respect to increasing concentric circle radii at various urban hierarchical levels: the city proper of Guangzhou, Guangzhou metropolitan region, and the

Pearl River Delta (PRD). For all regression curves and equations, the significance level P values < 0.001.

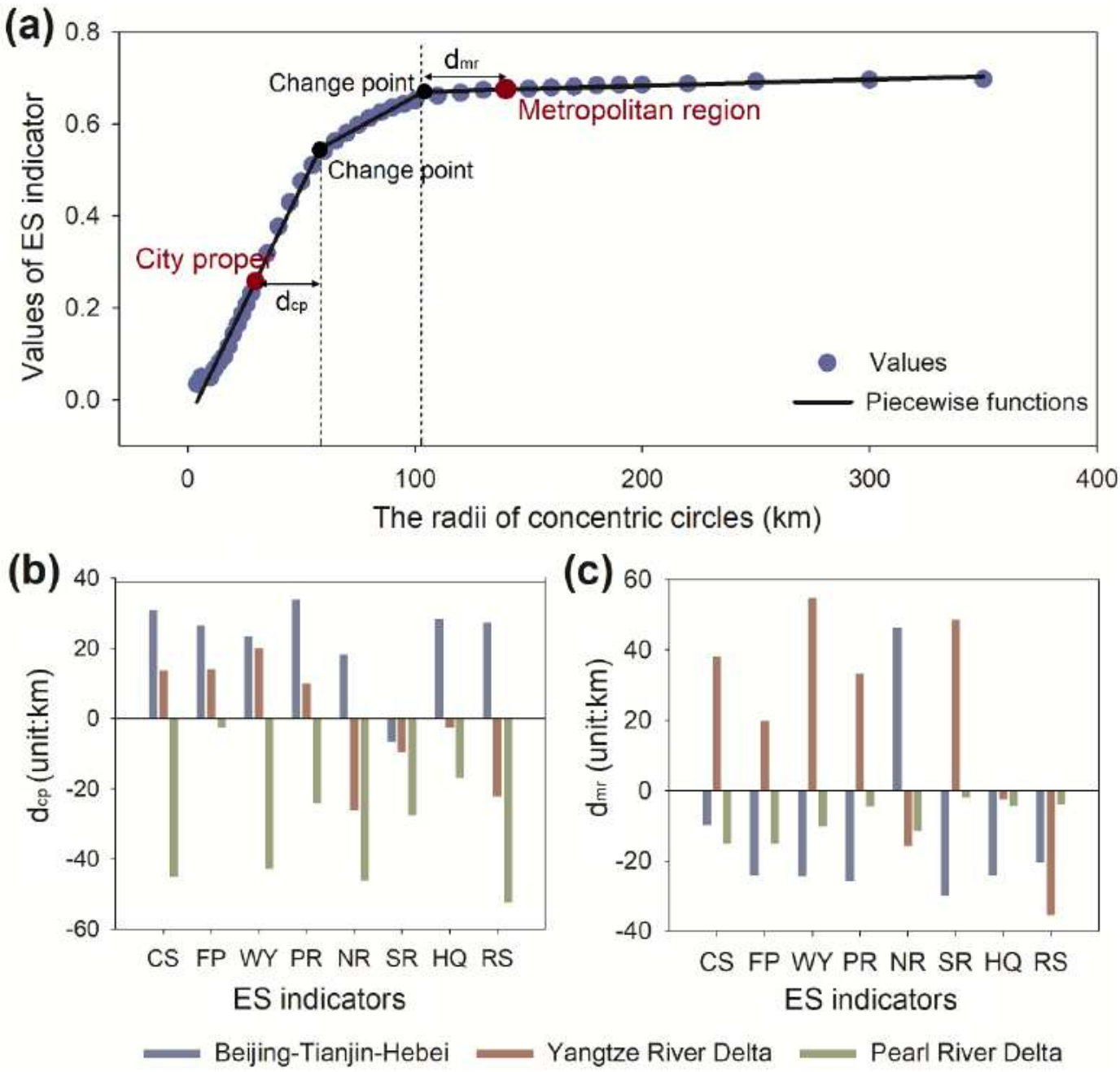

Figure 10

(a) Example of a scalogram for ecosystem service (ES) change points versus the administrative boundary points. The solid black dots represent the turning points for the ES change rates; the solid red dots represent the administrative boundary points. The “dcp” represents the distance between the first change point of ES scaling relations and the administrative boundary of the city proper; the “dmr” represents the distance between the second change point of ES scaling relations and the administrative boundary of the metropolitan region. Distance was calculated by the change point value minus the administrative boundary value. (b) The “dcp” for multiple ESs in Beijing Tianjin Hebei (BTH), Yangtze River Delta (YRD), and Pearl River Delta (PRD) urban agglomerations. CS = carbon storage; FP = food

production; WY = water yield; PR = PM2.5 removal; NR = nitrogen retention; SR = soil retention; HQ = habitat quality; RS = recreational opportunity. (c) The “dmr” for multiple ESs in BTH, YRD, and PRD urban agglomerations.

Supplementary Files

This is a list of supplementary files associated with this preprint. Click to download.

- SupplementaryInformationSI.docx
- Supplementaryfigures.docx